Authors' submitted manuscript (preprint)
Article published in Journal of Building Engineering, Vol. 97, 2024.
The final published version available at https://doi.org/10.1016/j.jobe.2024.110796

Valorization of coffee cherry waste ash as a sustainable construction material

Balasubramanya Manjunath [1], Claudiane M. Ouellet-Plamondon [2], Anjali Ganesh [3], B B Das [4], Chandrasekhar Bhojaraju [1*]

[1] Department of Civil Engineering, St. Joseph Engineering College, Vamanjoor, Mangaluru, Karnataka, India. 575028.

[2] Department of Construction Engineering, University of Quebec, École de technologie supérieure (ÉTS), 1100 Notre-Dame West, Montréal, QC, H3C 1K3, Canada.

[3] Department of Business Administration, St. Joseph Engineering College, Vamanjoor, Mangaluru, Karnataka, India. 575028.

[4] Department of Civil Engineering, National Institute of Technology Karnataka, Surathkal, India.

[*] Corresponding author: chandrasekhar.b@sjec.ac.in

Highlights

- Coffee cherry waste (CCW), a byproduct of coffee processing, was treated and investigated as a potential sustainable material to partially replace cement.
- Incorporating treated CCW up to 15% replacement of cement improved the compressive strength of mortar at all curing ages.
- Hydration studies showed that treated CCW enhanced cement hydration and led to a denser microstructure.
- Sustainability assessment revealed that incorporating treated CCW significantly improved the environmental performance.
- A fishbone diagram was developed to identify the potential challenges in the development and application of treated CCW in cementitious composites.

25

Graphical Abstract

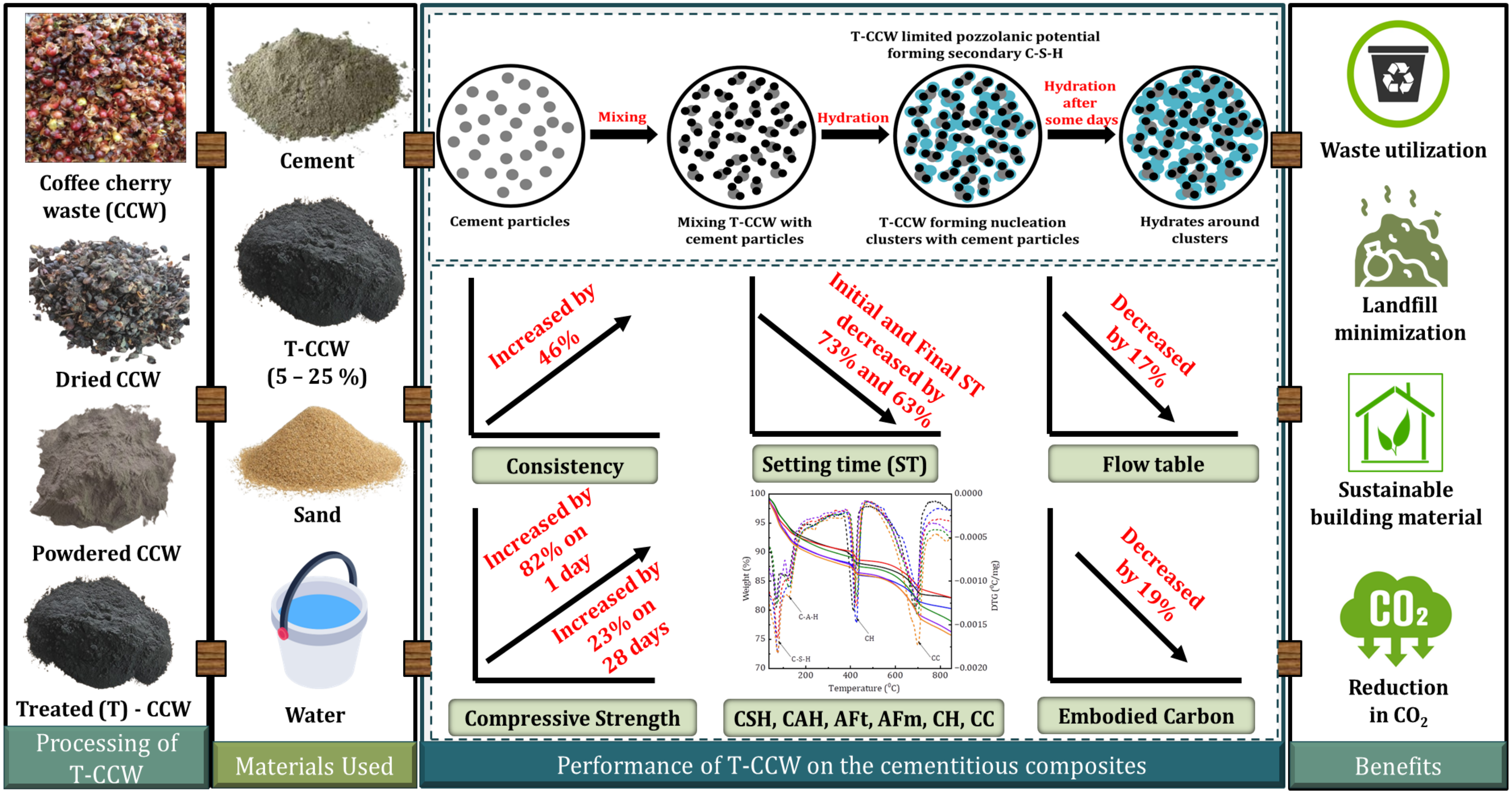

Authors' submitted manuscript (preprint)
Article published in Journal of Building Engineering, Vol. 97, 2024.
The final published version available at https://doi.org/10.1016/j.jobe.2024.110796

Abstract

This study explores the potential of treated coffee cherry waste (T-CCW) as a partial replacement of cement in mortar. T-CCW was characterized and incorporated into pastes and mortars at 5% to 25% cement replacement. The main objectives were to examine the fresh and hardened properties, hydration, and environmental assessment. Results showed that the high specific surface area and porous structure of T-CCW particles increased water demand and accelerated setting times. T-CCW incorporation of up to 15% enhanced compressive strength at all curing ages due to improved hydration and limited pozzolanic reactions. Ultrasonic pulse velocity indicated good homogeneity and compactness in T-CCW blended mortars. Microstructural analysis revealed that T-CCW enhanced cement hydration, leading to a denser matrix. Environmental analysis showed a reduced embodied carbon and cement intensity index compared to the control mix. Overall, the optimal performance was observed at 15% T-CCW replacement, significantly improving engineering properties and environmental impact. Further, the fishbone diagram addresses various factors to optimize the use of T-CCW as a cementitious composite. These findings demonstrate the potential of T-CCW as a sustainable construction material, offering a promising pathway towards environmentally friendly and resource-efficient building practices while addressing waste management in the coffee industry.

Keywords: Treated coffee cherry waste, Waste management, Strength, Hydration, Sustainability.

1. Introduction

The excessive production of anthropogenic carbon dioxide (CO_2) emissions seriously threatens ecosystems, and the damage caused by these emissions is immutable [1]. Anthropogenic activities that lead to this problem involve various processes, such as the use of fossil fuels for energy generation and the production of ordinary Portland cement (OPC) [2]. The production of OPC is responsible for approximately 7-8% of worldwide greenhouse gas emissions, making it one of the construction industry's most environmentally impactful materials [3]. Various strategies have been employed to reduce CO_2 emissions from cement production: a) improving energy efficiency, b) substituting fuels, c) implementing carbon capture and storage technologies, d) promoting effective cement usage, and e) using supplementary cementitious materials (SCMs) [4, 5]. The improvement in cement production through certain strategies may be limited due to the need for specialized equipment requirements, leading to higher costs [6, 7]. However, using SCMs as a replacement for OPC provides a viable alternative due to the economic benefits of using locally sourced materials and the potential for large-scale production. Industrial and agricultural wastes are feasible alternatives for cement binders.

Agricultural waste ashes have been extensively studied as SCMs to enhance the sustainability and performance of cement-based materials. Various sources, including walnut shell ash (WSA) [8], oat husk ash (OHA) [9], pistachio shell ash (PSA) [10], banana leaf ash (BLA) [11], wheat straw ash (WSA) [12], barley straw ash (BSA) [13], palm oil fuel ash (POFA) [14], rice straw ash (RSA) [15], bagasse ash (BA) [16], rice husk ash (RHA) [17], corn cob ash (CCA) [18], corn stover ash (CSA) [19], etc., have shown promising results. These materials exhibit diverse effects on cement properties. For instance, WSA improves pozzolanic activity, setting time, and long-term strength by promoting fibrous calcium silicate hydrate (C-S-H). OHA, calcined at 600 °C, can replace up to 20% of OPC without compromising strength. PSA enhances workability, setting time, and at 10% replacement, yielding a 17% increase in strength. BLA and WSA contribute to increased strength, with BLA reducing water absorption and WSA enhancing the microstructure of cement concrete. BSA optimizes the pore structure of concrete, leading to significant improvement in strength up to 15%. POFA in nano size can improve the compressive strength up to 30% without any reduction in strength. RSA, BA, and RHA contain significant amounts of silica, improving workability, strength, and durability. Untreated CCA presents challenges due to its high potassium content, but pretreated CSA enhances silica content, accelerating hydration and improving strength. The environmental benefits of these SCMs are significant, reducing landfill waste, lowering CO_2 emissions, and recycling agricultural waste into valuable construction material. However, each material's performance depends on its composition, processing conditions, and percentage of cement replacement, highlighting the need to optimize their application in cementitious composites. While significant progress has been made in this research, many agricultural wastes remain underutilized. This research explores coffee cherry waste (CCW) as a novel, sustainable alternative for construction materials, contributing to the enduring efforts to develop more environmentally friendly building practices.

The utilization of agricultural waste proves to be a cost-effective alternative compared to industrial waste [20]. Despite its application in various industries, disposing of agricultural waste through burning in open fields or using methods like stacking or landfilling can negatively impact the environment. Improper waste management and by-products can lead to soil degradation and water pollution. Also, landfill disposal leads to methane gas emissions, which are significantly more potent than CO_2, regarding their impact on global warming [21]. Thus, recycling and reusing waste can benefit the environment, economy, and society [22].

Globally, coffee is considered a highly significant commodity, widely traded, and the most consumed beverage [23]. The coffee industry significantly impacts the global economy, with Brazil, Vietnam, Colombia, Indonesia, India, Ethiopia, and Honduras being the biggest coffee producer countries, representing about 80% of global production [24]. It is concerning to note that coffee consumption and waste generation have increased simultaneously. During coffee production, a considerable amount of waste is generated, with 45% of the coffee plantation left as residue [25]. Also, during the washing process, a large quantity of water becomes contaminated and carries excessive carbon, which can harm the environment [26]. The technique used to process coffee can generate by-products throughout the various stages of processing, including pre-roasting coffee, dry processing (coffee cherry waste), semi-dry and wet processing (coffee pulp), and post-roasting coffee (coffee silverskin and spent coffee grounds) [27]. Fig. 1 shows the steps involved in the coffee processing using the west post-harvesting method.

Coffee cherry waste (CCW) is the non-usable part of the coffee beans and is the by-product primarily obtained through the wet method during coffee processing [28]. These wastes cover the coffee beans for approximately 12% of the cherry's dry weight [29]. It has been reported that for every tonne of coffee processed, the coffee processing industry produces approximately 0.18 tonnes of CCW [30]. The coffee cherries are taken to a processing facility where the under-ripe and overripe cherries are separated and treated accordingly. The seeds are then extracted from the cherries using a de-pulping machine. Approximately 90% of the coffee cherry waste is often discarded into a compost pile or dumped in landfills or water bodies. The improper disposal of these coffee cherry waste poses significant environmental problems for the soil and water around the farmland due to its high acidity and high levels of caffeine, tannins, and other polyphenols [31]. These wastes can acidify the soil, making nutrients unavailable for crops. Additionally, the long-term release of caffeine into water bodies negatively impacts the aquatic environment. Further, decomposing coffee cherries releases toxic mycotoxins that grow on coffee cherries, causing negative effects on the central nervous, cardiovascular, and respiratory systems [32]. The steps involved in generating CCW are shown in Fig. 2.

With an estimated increased production of coffee in the future, waste management policies for CCW must be implemented for proper handling and application, contributing to a circular and sustainable economy. Studies have investigated the possibility of using spent coffee grounds, but significant research has yet to be done on utilizing CCW as a construction material. This motivated the exploration of the potential of CCW as an alternative construction material to address the significant environmental challenges associated with cement production and the improper disposal of this byproduct.

According to the literature, more research is needed on the possible utilization of CCW as a substitute for cement. It is clear from previous studies that processing methods like burning and grinding significantly impact reactivity [33]. Hence, this research explores the possibility of using treated coffee cherry waste (T-CCW) for normal-strength mortar application. The following objectives were studied to investigate the feasibility of utilizing T-CCW as a construction material.

i) To perform an in-depth material characterization of T-CCW.
ii) To investigate the effect of T-CCW on cement paste and mortar properties.
iii) To study the effect of T-CCW on the hydration of cement paste.

An extensive experimental program has been carried out to answer these objectives. Different microstructural analyses are performed to investigate the characterization of T-CCW by a) X-ray diffraction (XRD), b) Thermogravimetric analysis (TGA), and c) Scanning electron microscopy (SEM), d) Energy dispersive spectroscopy (EDS) e) Fourier transform infrared spectroscopy (FTIR). Modified Chapelle tests were performed to assess the pozzolanicity. For the fresh properties of the T-CCW paste, tests such as a) consistency, b) setting time, and c) mini-slump flow are considered. The study investigates the hardened properties of T-CCW mortar. The hydration characteristics of T-CCW paste are conducted using SEM, XRD, TGA, and FTIR. A fishbone diagram is drawn to identify, analyze, and display the potential causes of using T-CCW in cement.

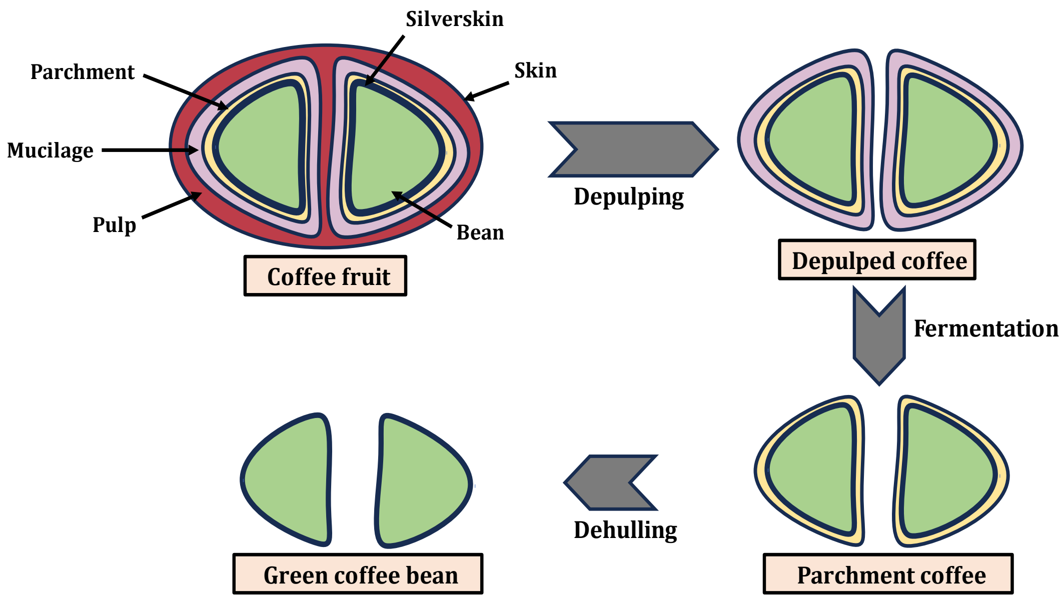

Fig. 1. Steps involved in the coffee processing using the west post-harvesting method

2. Materials and methods

2.1 Materials

2.1.1 Cement and Fine Aggregate

The commercially available OPC of 53 grade conforming to IS 12269 is utilized in the present study. The chemical composition of OPC is shown in Table 1. The normal consistency is 29%, the specific gravity is 3.14, 160 min initial setting time and 310 min final setting time, and the specific surface area of OPC was 365 m^2/kg. Natural river sand was used as a fine aggregate. The sand was washed, sundried, and sieved. The fine aggregate used in this study is categorized as zone 2, passing through a 2.36 mm sieve and retained on a 150 μm sieve. The water absorption, specific gravity, and fineness modulus were 0.95 %, 2.68, and 2.50, respectively.

2.1.2 Treated coffee cherry waste

The CCW used in the study is collected from the Chikkamagaluru district, Karnataka, India. Once coffee seeds are extracted, the leftover cherry is often discarded in landfills or water, leading to environmental issues like soil and water pollution. The CCW was collected from the disposal site, sun-dried for 7 days, and then dried in an oven at 105°C for 24 h to remove moisture. After cooling, the dried CCW was pulverized and grounded in a laboratory ball milled for 1 h at 60 rpm using stainless steel balls with a ball-to-powder ratio of 10:1. These specific durations and speeds were chosen to achieve the optimal particle size reduction. The SEM image of the grounded CCW is illustrated in Fig. S1. Later, the milled CCW was calcined at 550°C for 30 min [34]. This temperature was selected based on the thermogravimetric analysis (TGA) results for the grounded CCW. The TGA curve of the grounded CCW is presented in Fig. S2. At this temperature, all the thermal decomposition processes have been completed, eliminating most of the organic matter, and the rate of weight loss has decreased, indicating a stable carbon structure. The duration of 30 min allows for complete thermal treatment and ensures uniform carbonization throughout the resulting material while minimizing the increase in the ash content. After cooling, the calcined CCW was sieved using a 75 µm sieve [35, 36]. This size was chosen to ensure uniformity in particle size distribution. Also, the reactivity of any material is often linked to its fineness. Finer particles have a larger surface area, which enhances their reactivity. The step-by-step procedure for T-CCW is illustrated in Fig. 3. The chemical composition of T-CCW is indicated in Table 1. The T-CCW exhibited a specific gravity of 2.12 and the Blaine's specific surface area of 914 m^2/kg. The size distribution of T-CCW particles is analyzed with a laser diffraction particle size analyzer, shown in Fig. 4. It confirms that the D10 (i.e., the diameter of the particles at 10% passing), D50, and D90 values of T-CCW are 3.03 µm, 19.21 µm, and 53.99 µm with mean particle size 24.66 µm.

Table 1 Chemical composition of OPC and T-CCW

Oxides (%)	OPC	T-CCW
SiO_2	19.15	28.65
Al_2O_3	5.67	10.30
Fe_2O_3	4.87	10.72
CaO	63.25	11.77
MgO	1.56	1.8
SO_3	2.26	2.64
Na_2O	0.35	0.22
K_2O	0.53	11.88
P_2O_5	0.11	3.01
LOI	1.13	18.75

2.2 Mix proportions

Five mixes of T-CCW were prepared and investigated to study the impact of T-CCW on pastes and mortars. The mix proportions of pastes and mortars used in the study are given in Table 2. In this study, the water-to-binder ratio of 0.48 and sand-to-binder ratio of 2.75 were selected based on the trial mixes to achieve a workable consistency and optimal performance of mortar mixes. [20]. The variation of T-CCW replacement from 5% to 25% at 5% intervals was chosen to systematically investigate the effect of incremental additions on the fresh and hardened properties, providing a comprehensive understanding of the material's potential as a sustainable cement replacement. The reference is labelled as C0 and the other C5, C10, C15, C20, and C25, respectively. Based on the mixture proportion, the fresh and hardened characteristics of pastes and mortar are conducted.

2.3 Preparation of mixtures

Cement paste was prepared using a high-speed stirrer, IKA RW 20, with a max speed of 2000 rpm. In the first stage, dry materials are mixed at 200 rpm for 60 s. Water is added to the mixture and mixed for 60 s at 500 rpm. The paste is left to rest for 90 s in the next stage before being continuously mixed for 90 s at 1500 rpm in the final step. Mortar mixes were prepared using a standard Digi mortar mixer. Initially, all materials (cement, sand, T-CCW, and water) are manually mixed. The materials are mixed at low speed for 60 s, then 30 s at high speed. The mortar mixer rests for 90 s to clean the sides of the bowl before being mixed for another 60 s at high speed [20]. Each mortar mix was kept at a flow value of 110 ± 5 mm or higher. The mortar mixture was poured into cube-shaped moulds measuring 50 mm and 70.7 mm, respectively. The moulds were vibrated to remove entrapped air, filled with the mixture, and left for 24 h. They were then placed in a curing tank for water curing. Various tests were conducted at the respective ages.

2.4 Testing of samples

The flowchart of the experimental program is illustrated in Fig. 5.

2.4.1 Characterization of T-CCW

X-ray fluorescence (XRF) was used to analyze the sample's chemical composition. XRD is a method to examine the crystallographic structure of materials. The microstructure of the sample was analyzed using SEM. TGA is a thermal analysis technique used to study changes in sample weight as temperature increases under controlled conditions. FTIR is an analytical method that uses infrared absorption and emission spectra to identify and analyze the chemical composition of substances.

2.4.2 Tests on pastes, fresh and hardened properties of mortars

The Vicat apparatus was used to determine the standard consistency and setting times of cement paste samples for both control and T-CCW, following IS 4031- Part IV and V. The mini-slump cone test measured the flow of fresh cement paste by lifting the filled cone and measuring the increase in its diameter in perpendicular directions [37]. All the mortar mixes were prepared using a Digi mortar mixer according to IS 2250-1981. The mixer was used to mix fine aggregate, Portland cement, T-CCW, and water. After mixing, the flow table test was conducted in accordance with IS 4031 (Part 7)-1988. The mortar was placed on the table, and the flow was recorded by measuring the spread diameter of each mixture after 25 drops. The compressive strength of mortar was measured using 50 mm cubes that were water-cured for 1, 3, 7, and 28 days. Vertical axial loading was applied, and the maximum load was recorded to calculate the compressive strength. Ultrasonic pulse velocity (UPV) is a non-destructive testing method that measures pulse velocity to evaluate properties such as homogeneity, cracks, and voids in hardened mortar. The mortar cubes, measuring 70.7 mm, are tested for UPV using a PUNDIT portable device.

2.4.3 Hydration Studies of T-CCW

The pastes were moulded and stored in lime water to prevent leaching. XRD, TGA, FTIR, and SEM studies were performed on 7-day hydrated cement paste samples. The samples were treated with isopropanol and diethyl ether to stop the hydration process and stored free from carbonation until tested. Samples were taken from the interior of the crushed specimens for SEM analysis. The specimens were ground and sieved through a 75 µm sieve for XRD, TGA, and FTIR. For TGA, the weight loss was then monitored from 30 to 900 °C, with a heating rate of 10 °C/min. The amount of calcium hydroxide or portlandite (CH) present in cement samples can be determined using Eq. (1) [11].

$$CH = \frac{(W400 - W500)}{W500} \cdot \frac{74}{18} \cdot 100 \qquad (1)$$

Based on previous studies, bound water (BW) was determined using Eq. (2) [11]. The higher BW indicates a more significant formation of hydrates [38, 39].

$$BW = \frac{(W40 - W500)}{W500} \cdot 100 \qquad (2)$$

W40, W400 and W500 – Weight loss at 40 °C, 400 °C and 500 °C. The breakdown of hydrates can be separated into three main stages. The initial stage, below 400 °C, includes the disintegration of hydrates. The second stage, between 400 to 500 °C, is mainly dominated by the dehydroxylation of CH. The third stage is characterized by the decarbonization of calcite (CC) [40]. For FTIR, pellets were created with 1 mg sample and 100 mg KBr, with spectra recorded in the wavenumber range of 4000–400 cm^{-1}. The crystalline phases present in the samples were evaluated through XRD in the 2θ range of 10 – 80° for samples.

2.4.5 Environmental analysis and fishbone diagram

Sustainability assessment and the cement intensity index (CII) were calculated for the mortar mixes and the hardened properties of the mortar, followed by a fishbone diagram as an analytical tool examining the potential challenges associated with the use of T-CCW.

Fig. 2. Steps involved in generating CCW: 1) Coffee fruit 2) Harvesting of the coffee fruit 3) Washing coffee fruit 4) Depulping coffee fruit 5) Cherry waste dumped as landfill 6) Cherry waste dumped in the water bodies

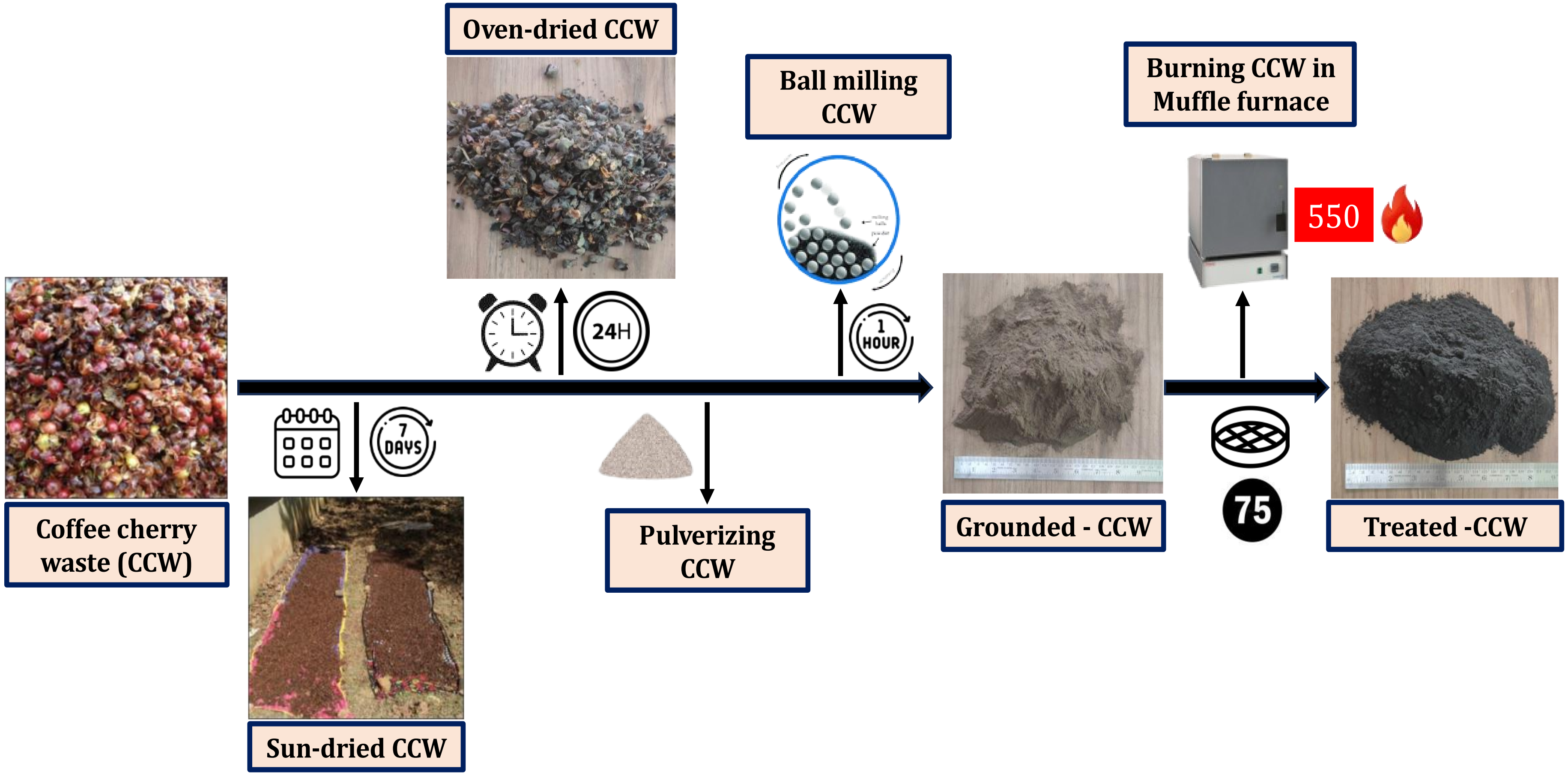

Fig. 3. Step-by-step procedure for the preparation of T-CCW

255

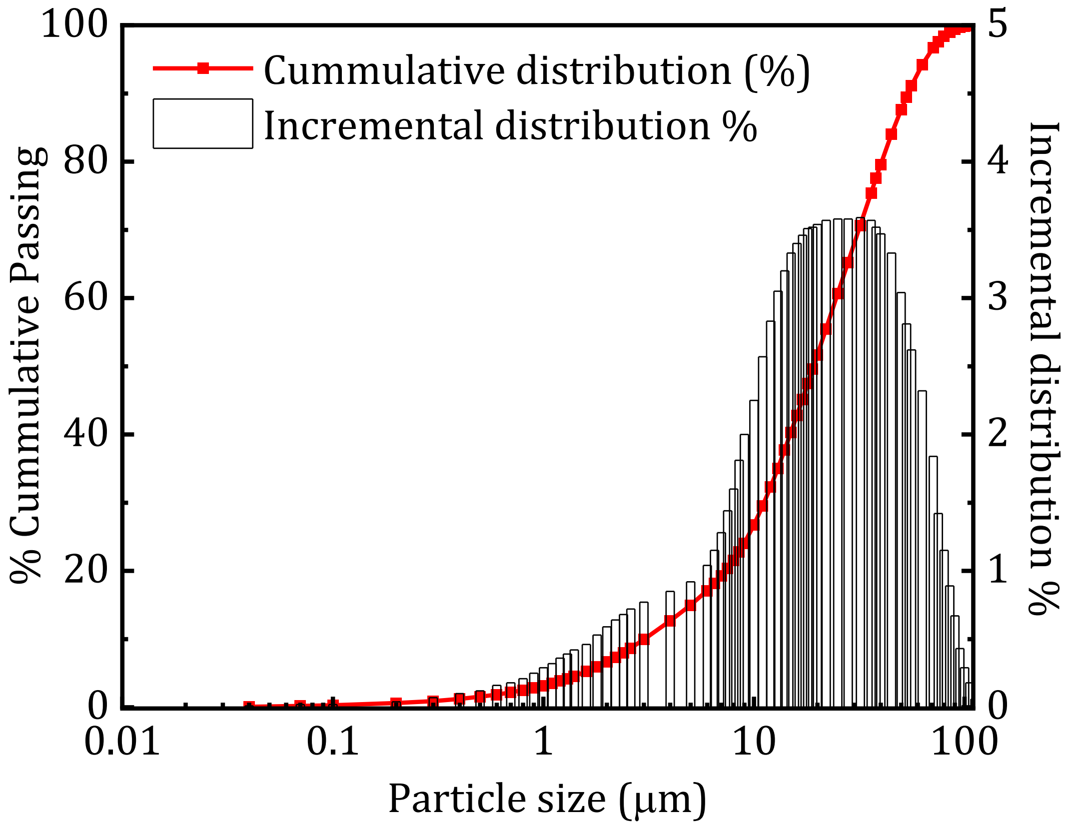

Fig. 4. Particle size analysis of the T-CCW

Table 2 Mix proportions of T-CCW – OPC based blended paste and mortar

Mixes	OPC (g)	T-CCW (g)	Water (g)	Sand (g)
C0	450.0	0.0	216	1237.5
C5	427.5	22.5		
C10	405.0	45.0		
C15	382.5	67.5		
C20	360.0	90.0		
C25	337.5	112.5		

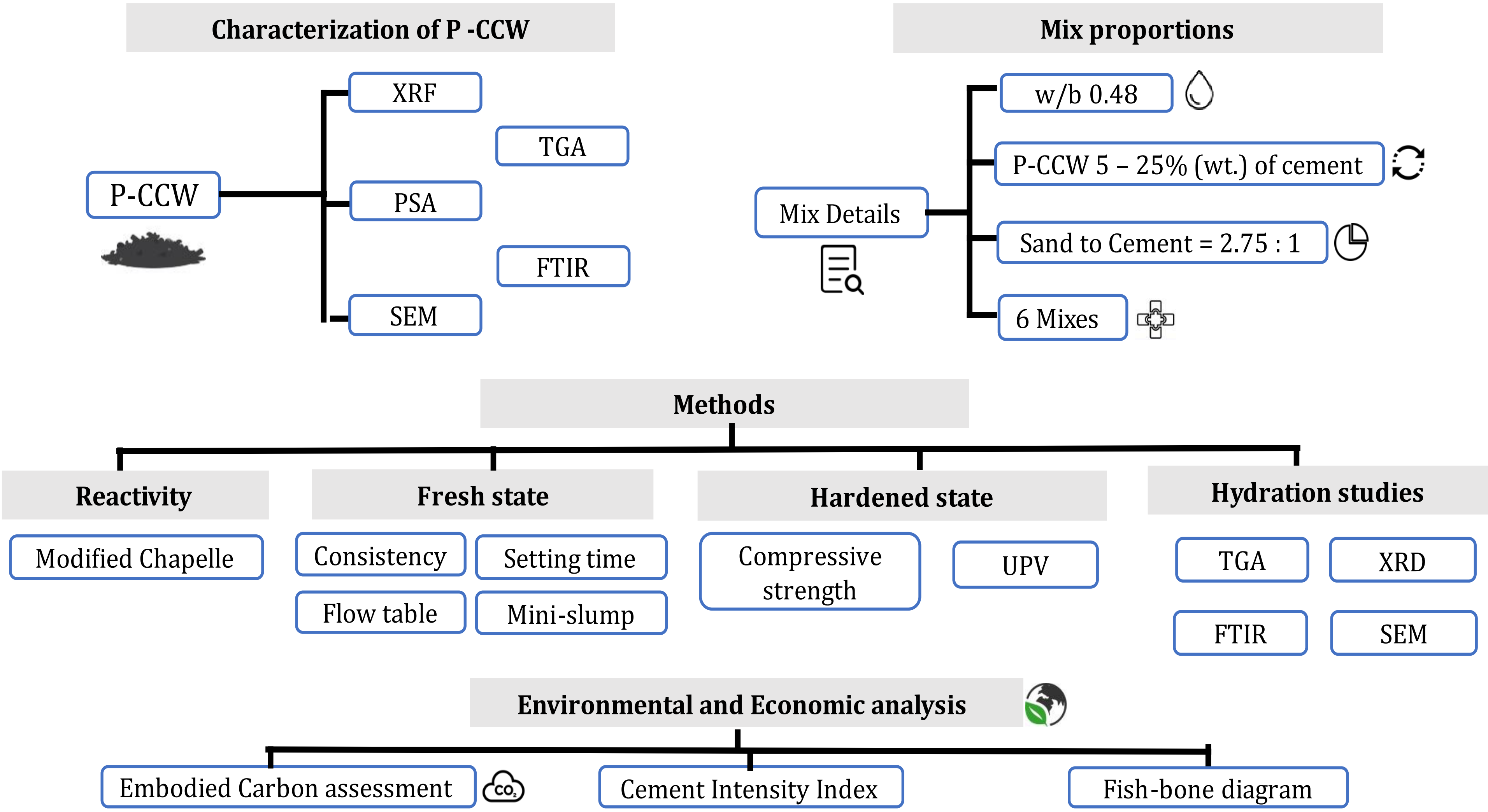

Fig. 5. Flowchart of the experimental program

3. Results and discussions

3.1 Characterization of T-CCW

The morphology of the T-CCW is studied by using SEM, as shown in Fig. 6(a). T-CCW particles exhibit irregular shapes with wrinkled and rugged surfaces [31, 41]. Further, T-CCW particles exhibit the presence of numerous pores on the surface, indicating the release of volatile and organic matter from the untreated CCW during the thermal decomposition process. These pores can absorb water and serve as an internal curing agent. The SEM of the untreated CCW is illustrated in Fig S1. The EDS analysis of the T-CCW is presented in Fig. 6(b).

The FTIR spectra of the T-CCW sample exhibit several peaks, indicating the presence of various functional groups. The broad peak at 3300 cm^{-1} is attributed to the stretching vibrations of O-H groups [42], suggesting the presence of phenolic hydroxyl groups in the T-CCW sample. The peak at 2986 cm^{-1} is assigned to the C-H stretching vibration of methyl groups present in organic compounds such as proteins, lignin, and cellulose. These peaks may indicate the presence of caffeine [43]. The absorption band at 1420 cm^{-1} corresponds to the bending vibration of C-H bonds in methyl groups [44]. The peak at 1020 cm^{-1} is associated with the stretching vibration of C-O groups in the C-O-H glycosidic bonds, which are characteristic of galactomannans, a class of polysaccharides present in the CCW [45]. The peak at 874 cm^{-1} is attributed to the stretching vibrations of the C-O-C glycosidic bonds, further confirming the presence of polysaccharides in the sample [46]. The band at 764 cm^{-1} indicates the presence of aromatic C-H deformation vibration [47], suggesting the presence of aromatic compounds derived from lignin and other aromatic components in the CCW.

TGA was employed to investigate the thermal decomposition characteristics of T-CCW. The TG-DTG curves in Fig. 7(b) show three distinct thermal degradation zones. The first zone, ranging from 30 to 190 °C with a peak at 55 °C, corresponds to the evaporation of surface-bound water [31], resulting in approximately 3% weight loss. The second zone, ranging from 190 to 500 °C, represents the decomposition of major organic compounds in T-CCW. While no prominent peaks were observed in this region, a peak at around 440 °C suggests significant cellulose content and the beginning of the lignin decomposition. Typically, hemicellulose decomposition occurs between 200 to 300 °C. cellulose between 300 to 400 °C, and lignin decomposition initiates at approximately 400 °C, extending to higher temperatures [48]. The third zone, ranging from 500 – 900 °C with a peak at 660 °C, is attributed to the endothermic degradation of lignin [49] and the breakdown of thermally stable organic compounds [50]. The shift of this peak towards higher temperatures indicates enhanced thermal stability of the material at elevated temperatures.

a)

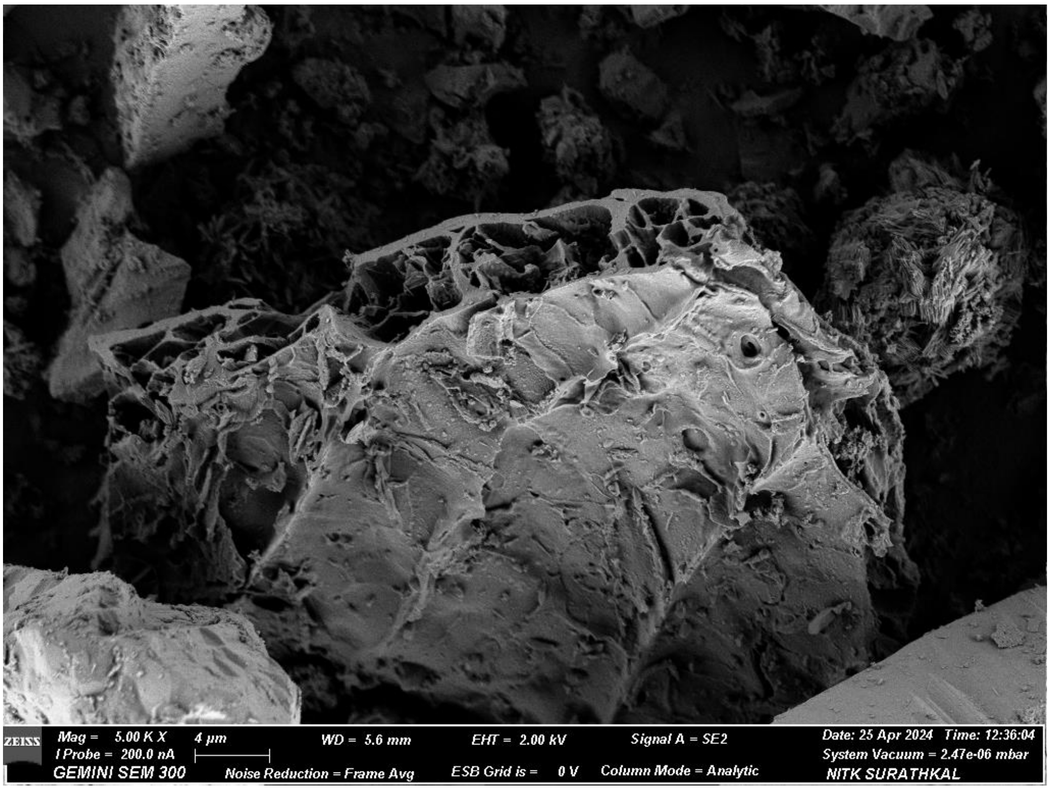

b)

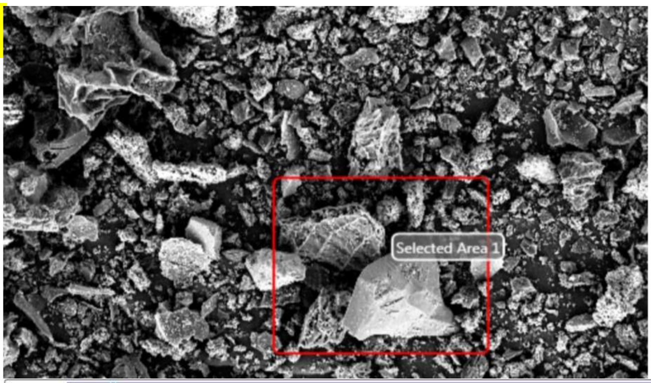

Element	Wt. %	At %
C K	43.19	56.80
O K	29.18	28.81
Al K	1.50	0.88
Si K	18.63	10.48
K K	7.49	3.03

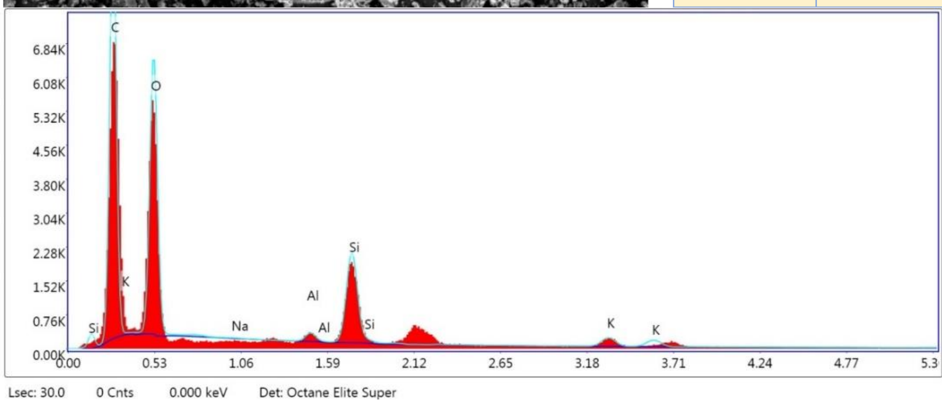

Fig. 6. a) SEM b) EDS of the T-CCW

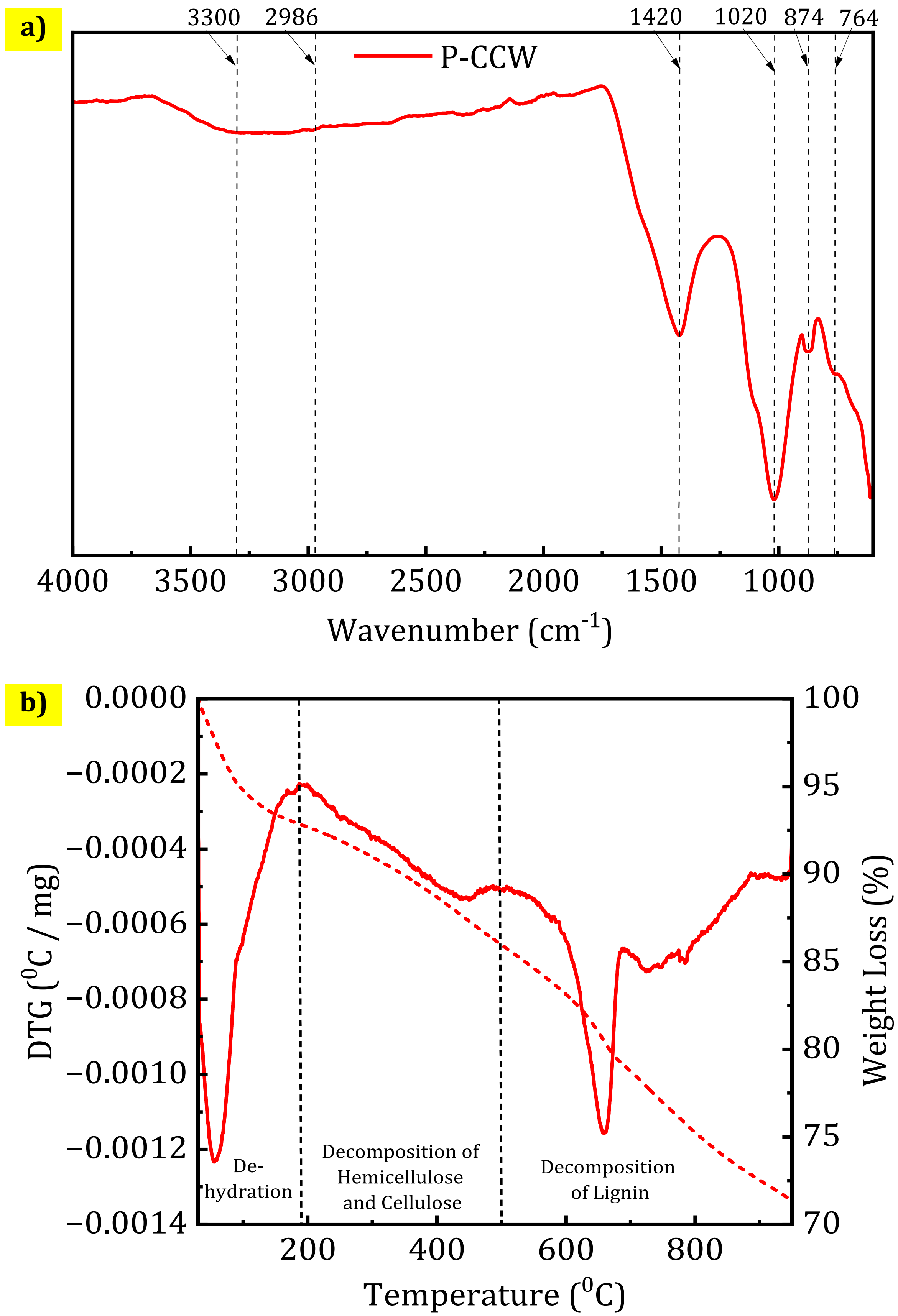

Fig. 7. a) FTIR b) TGA of T-CCW

3.2 Modified Chapelle test to evaluate the reactivity of T-CCW

The Chapelle activity test is a chemical method to measure the fixed quantity of calcium hydroxide on pozzolanic materials to define their pozzolanic activity. The procedure to conduct the modified Chapelle test is as per NF P 18-513 standards [51]. Fig illustrates the steps carried out for the Chapelle test of T-CCW. Using the formula given in eqn

$$\text{Amount of Ca (OH)}_2 \text{ fixed} = 2 \times ((V_1 - V_2) / V_1) \times (74/56) \times 1000$$

Where V_1 is the volume of 0.1N HCl obtained by blank, which is equal to 9.4, and V_2 is the volume of 0.1N HCl obtained by the reaction of the T-CCW, which is equal to 9.0. The Ca $(OH)_2$ fixed for T-CCW is 112 mg of Ca $(OH)_2$/g. This indicates that T-CCW consumes less CaO than traditional SCMs like fly ash, which typically shows around 666 mg of Ca $(OH)_2$/g [52]. Based on the results of the Chapelle test, T-CCW cannot be classified as a traditional SCM due to its significantly lower CaO consumption compared to conventional SCMs like fly ash, slag, or silica fume. However, T-CCW demonstrates some pozzolanic properties that contribute to cementitious mixtures. Therefore, T-CCW can be proposed as an alternative sustainable material with unique characteristics that exhibit lower pozzolanic potential and can act as a filler material.

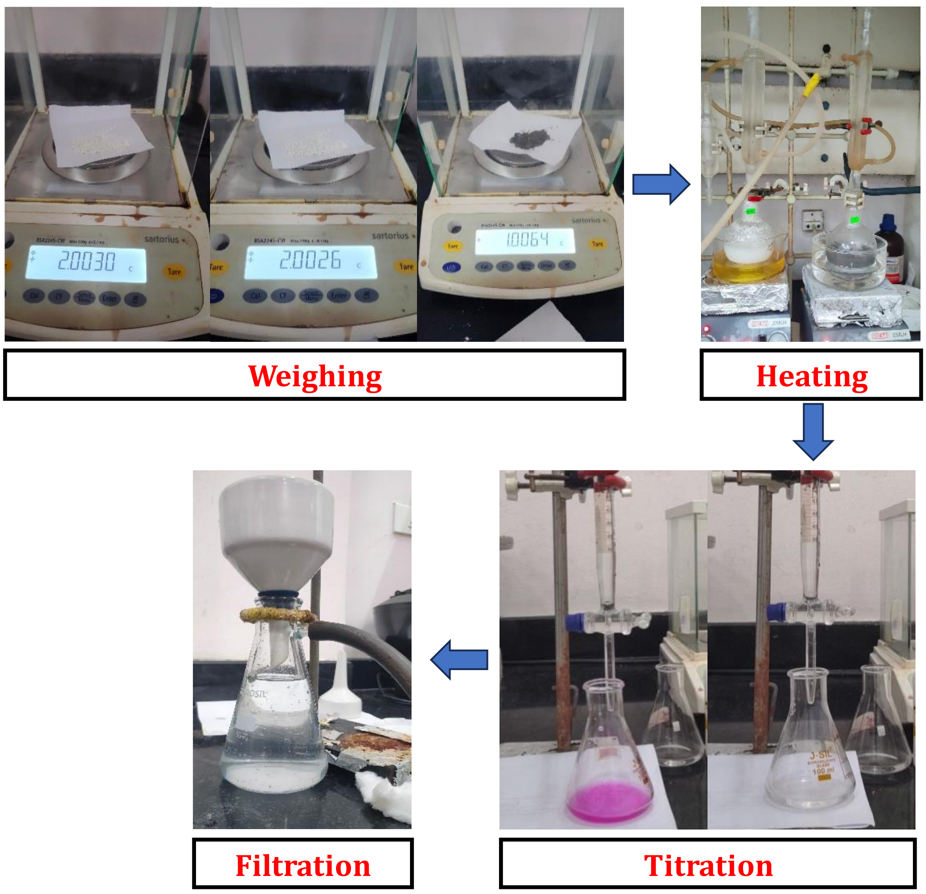

Fig. 8. Experimental setup for Modified Chapelle test.

3.3 Normal Consistency

The consistency of the blended cement pastes incorporating T-CCW was determined by the percentage of water demand, according to the replacement levels of T-CCW, as shown in Fig. 9. The control mix exhibited a consistency of 28.5%. As the T-CCW replacement levels increased, the water demand for achieving consistency progressively increased to 29%, 31.5%, 33%, 38.5%, and 41.5%, respectively. The water requirement for the consistency of the blended cement pastes increased up to 46% compared to the control mix. This significant increase in the water demand for T-CCW blended cement pastes can be attributed to the porous nature of the T-CCW particles, as evidenced by the SEM images in Fig. 6(a). The porous structure of T-CCW particles allows them to retain water within their pores, effectively reducing the free water available and necessitating additional water to maintain the desired consistency [53]. The results of using other biomass ashes have also increased the water demand for the blended cement pastes [10, 20].

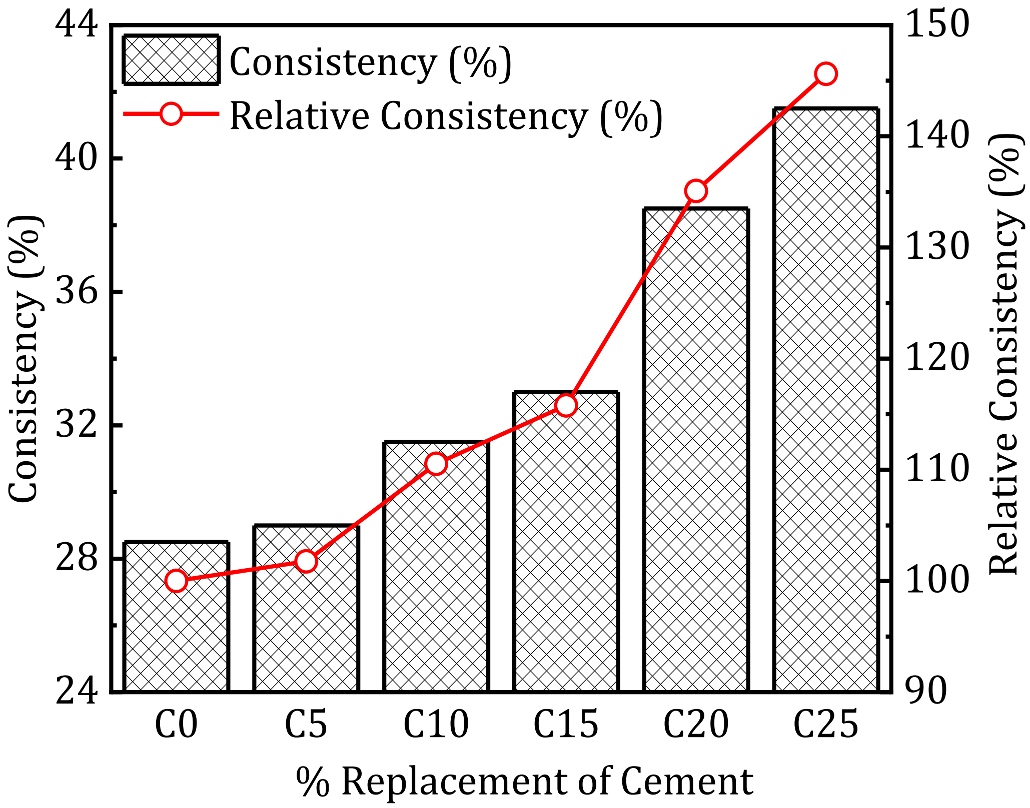

Fig. 9. Consistency of the blended cement

3.4 Setting time

The hydration process is responsible for the setting of the cement paste. The initial and final setting times for various percentages of T-CCW were measured using Vicat's apparatus, and the results are shown in Fig. 10. The experimental results showed that the increase in the percentage of T-CCW leads to a substantial reduction in the initial and final setting times of the blended cement pastes. The addition of 25% T-CCW resulted in a 73% and 63% decrease in the initial and final setting times compared to the control cement paste. This behaviour can be attributed to three mechanisms. (i) The high surface area and porous structure of T-CCW material provide nucleation sites for the formation of hydration products, and the water retention capacity of the T-CCW within the pore structure ensures a continuous supply of water, maintaining the hydration reactions and contributes to faster setting times [54]. (ii) The higher alkali content in T-CCW has accelerated the hydration process, thereby affecting the setting time of the blended cement paste [55].

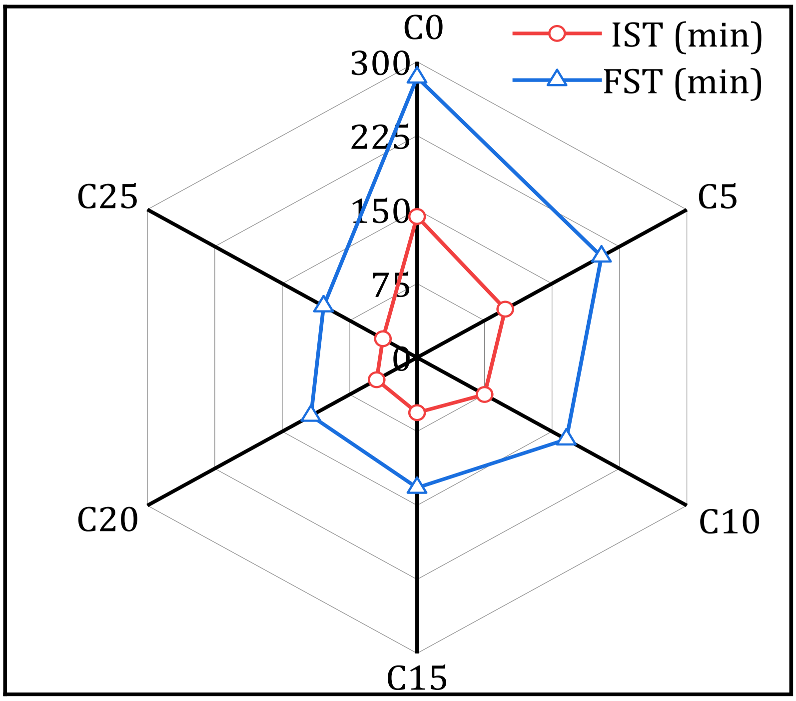

Fig. 10. Setting time of the blended cement

3.5 Mini slump flow and Flow table

The relationship between the percentage of T-CCW content and mini-slump flow is illustrated in Fig. 11. The mini-slump diameter of the control paste was 142 mm at 0 min and decreased to 110 mm at 25 min. However, for the blended cement pastes, the results indicate that the increase in the percentage of T-CCW content reduced the mini-slump flow diameter at all the time duration. The significant water absorption, high specific surface area, and porous structure of T-CCW are attributed to the decrease in flowability [53].

Furthermore, a flow table test conducted on the mortar with varying percentages of T-CCW revealed that the flow table values decreased with the increase in T-CCW content, as presented in Table 3. The flow table value of the blended cement mortar decreased by 5%, 8%, 10%, 12%, and 17%, respectively, compared to the control mortar. The incorporation of T-CCW necessitates additional water due to its irregular geometry and porous nature, as observed by SEM, leading to lower flow values [56].

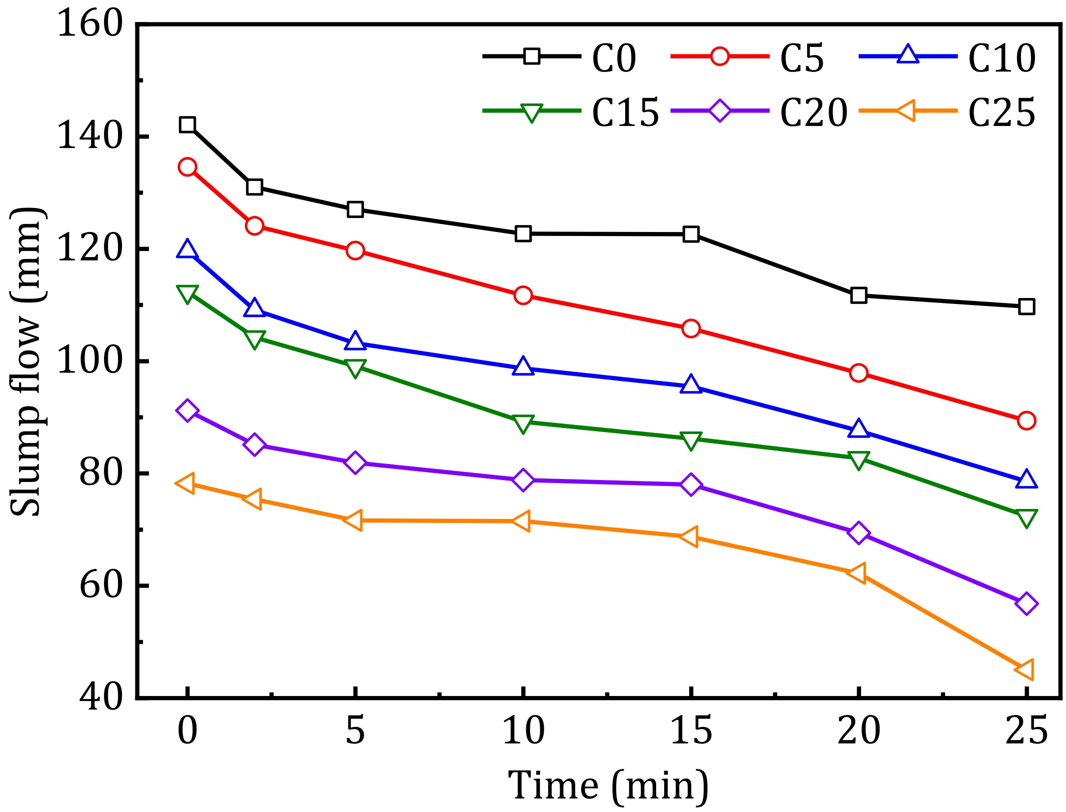

Fig. 11. Mini slump flow and flow table value of the blended pastes

Table 3 Flow table of the blended cement mortar

Mix	Flow table value (mm)
C0	155
C5	148
C10	143
C15	140
C20	136
C25	129

3.6 Compressive Strength

One of the critical parameters governing the structural viability of mortar mixes is compressive strength, which directly correlates to the load-carrying capacity. The compressive strength of the control and blended cement mortar samples incorporating T-CCW at various replacement levels was conducted at 1, 3, 7, and 28 curing days, as shown in Fig. 12. The influence of T-

CCW has a notable impact on the strength development of the mortar mixes. An increase in T-CCW percentage up to 15% in the mortar increases compressive strength compared to the control mortar at all the curing ages. The incorporation of 15% T-CCW yielded the highest compressive strength values of 13.6, 24.1, 32.6, and 45.1 MPa, exhibited an enhancement of 82%, 53%, 49%, and 23% compared to the control mortar at 1, 3, 7, and 28 days of curing, respectively. Firstly, the improved strength can be attributed to the larger surface area and porous and hydrophilic nature of T-CCW, which facilitates water absorption during mixing and subsequent release during self-desiccation, effectively completing the hydration process [57, 58]. Secondly, T-CCW favours the development of pozzolanic reactions, allowing secondary calcium silicate hydrate (C-S-H) gel formation. Additionally, the high alkaline content of T-CCW accelerates the hydration reaction, enhancing early strength in cementitious composites [59]. Further increasing the T-CCW content beyond 15% reduced strength, potentially due to the low-filling effect [60] and the increase in pores [61]. However, the compressive strength of all the mortar mixes was within the standard value specified by ASTM C270 and ASTM C90. Compared to T-CCW with other SCMs of similar mix proportion, 15% T-CCW blended cementitious composite achieved a 28-day compressive strength of 45.1MPa, which is comparable with the 20% fly ash replacement (42.7 MPa) reported by Siddique. [62]. However, a 30% GGBS replacement studied by Oner and Akyuz (2007) yielded a slightly higher strength of 47.5 MPa [63]. These comparisons highlight that T-CCW can achieve similar or better strength performance at lower replacement levels compared to other common SCMs because of its nucleation and limited pozzolanic effect.

In addition, a two-way ANOVA was employed to understand the influence of T-CCW percentage and concrete age on the strength, and the values are presented in Table S2. It is evident from the analysis that the T-CCW percentage ($F(5, 63) = 12.4$, $p < 0.0001$) and age of concrete ($F(3, 63) = 277.67$, $p < 0.0001$) have a significant influence on strength values.

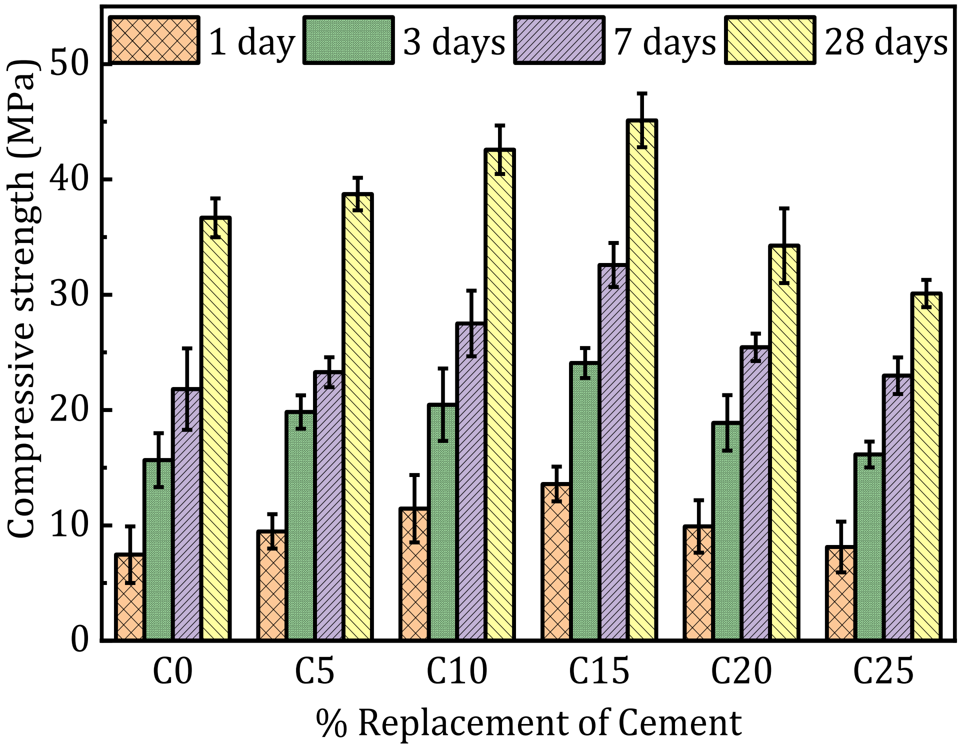

Fig. 12. Compressive strength of the blended cement

3.7 Ultrasonic pulse velocity

The UPV, a non-destructive method, was employed to evaluate the uniformity, homogeneity, and presence of voids or cracks in the hardened mortar specimens [20]. Fig. 13 illustrates the impact of T-CCW on the UPV values of the mortar at curing ages of 1, 3, 7, and 28 days. The UPV of the mortar ranged from 3258 to 3715 m/s on 1 day, 3459 to 4119 m/s on 3 days, 3724 to 4296 m/s on 7 days, and 3978 to 4525 m/s on 28 days. A notable increase in the UPV values is observed with the increase in the curing period. The C15 mix, exhibiting the highest compressive strength, also demonstrated the maximum UPV value, indicating a good correlation between UPV and the compressive strength of the mixes. This correlation suggests a positive influence of T-CCW on the homogeneity and compactness of the mortar matrix. The utilization of T-CCW causes a micro-filling effect, resulting in the development of additional nucleation sites and the development of secondary pozzolanic reactions that contribute effectively to the densification of the matrix [54]. However, higher replacement levels of T-CCW resulted in a less dense matrix with increased porosity. All the mortar mixes exhibited UPV values exceeding 3900 m/s at 28 days, indicating the mix is durable [64], and potentially advantageous for structural applications. The two-way ANOVA analysis showed that the percentage of T-CCW and curing age significantly affect UPV in concrete. Changes in T-CCW percentage had a strong effect ($F(5, 63) = 39.16$, $p < 0.0001$), meaning that even small changes in T-CCW amount can noticeably influence UPV. Curing time had an even more significant impact ($F (3, 63) = 133.61$, $p < 0.0001$. The overall model was very strong ($F (8, 63) = 74.58$, $p < 0.0001$).

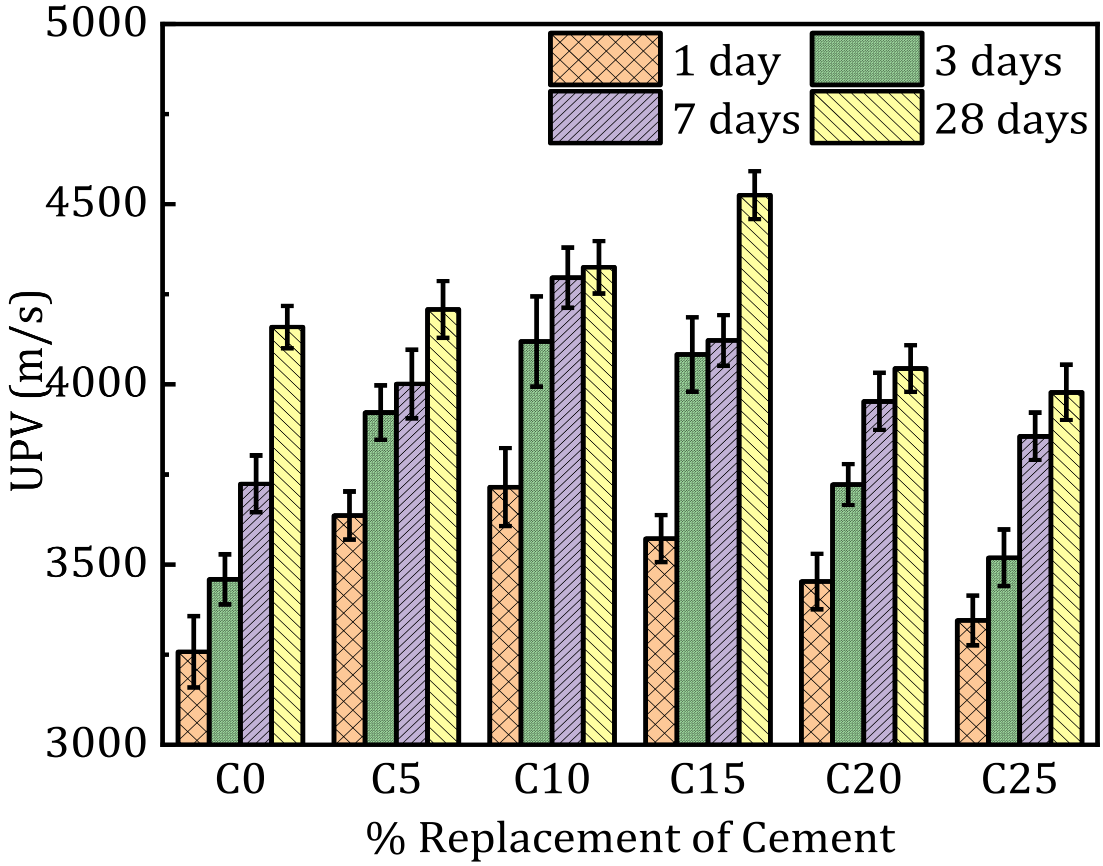

Fig. 13. UPV of the blended cement

4. Hydration studies

4.1 Scanning electron microscope

Fig. 14 presents the SEM images of C0, C10, and C25 pastes after 7 days. The SEM images show the formation of hydration products, such as the needle-shaped ettringite (AFt) crystals, distinctive hexagonal-prismatic crystals of portlandite (CH), and C-S-H gel. The T-CCW samples (C10 and C25) showed traces of monosulphate (AFm). The T-CCW admixed pastes exhibit a dense microstructure compared to control pastes, resulting in increased hydration products. The hydration process involves pore solution entering internal pores, facilitating the precipitation of hydration products within these pores [65], and the secondary pozzolanic reaction formed by the reaction of T-CCW with CH contributes to the strength development. Further, the fine particles of T-CCW act as nucleation sites, and the porous structure helps to retain water, ensuring continued hydration and the formation of a denser matrix [66]. As a result of these mechanisms, the SEM of the T-CCW blended pastes exhibits fewer voids compared to the control.

4.2 Thermogravimteric analysis

TGA-DTG was used to investigate the influence of T-CCW on the formation of hydration and carbonation products, as illustrated in Fig. 15(a). The three main peaks associated with the TGA curves are dehydration of C-S-H, calcium aluminate hydrate (C-A-H), Aft, and AFm (105 – 400 °C), dehydroxylation of CH (400 – 500 °C), and decarbonation (500 – 900 °C) [67]. The differential thermogravimetric (DTG) curve shows that the peak before 100 °C is attributed to the enhanced hydration product formation due to T-CCW, which absorbs water from the surrounding environment [65]. Also, the pozzolanic reactions facilitated the development of secondary hydrates to occur. The second peak (400 – 500 °C) corresponds to the decomposition of CH, which is directly related to the degree of cement hydration. The CH content directly from the DTG curves cannot be interpreted correctly; therefore, the percentage of CH and BW were quantitatively determined using Eq (1) and (2). The results of these calculations are presented in Fig. 15(b) to provide a clear understanding of the hydration process. The increase in T-CCW percentage resulted in a decrease in CH and an increase in BW. Despite the higher w/c ratio, the reduction in CH is not only due to the dilution of the cement content but also the secondary pozzolanic reaction between T-CCW and CH [11]. These findings agree with the compressive strength results at 7 days. The third peak (600 – 750 °C) resulted from the decomposition of CC, precipitated during the carbonation of C-S-H, and well-crystalline calcite formed from the carbonation of portlandite.

4.3 X-ray diffraction

The XRD patterns for the cement paste blended with T-CCW at 7 days are presented in Fig. 15(c). The results indicated that the incorporation of T-CCW enhanced the formation of hydration products. The main crystalline phases detected in all the samples are CH (P), CC (C), Tricalcium silicate (C_3S) (T), and Dicalcium silicate (C_2S) (D). The AFt and AFm phases are observed in T-CCW blended samples with higher replacement levels. The characteristic peaks of CH were identified at 18°, 34.08°, 47.08°, and 50.8°. The intensity of the portlandite peak at 18° was higher in blended cement paste up to 15% of T-CCW, which may be attributed to the limited pozzolanic activity of T-CCW [68] and the pores of T-CCW provided a favourable environment for the growth of hydration products [57]. The XRD patterns show less intense peaks at 32.2° and 41° for C_3S and C_2S, suggesting enhanced hydration kinetics. Furthermore, the CC peaks are observed at 23°, 29.4°, 39.4°, and 43.2°. The water absorbed by the pores of T-CCW facilitates the dissolution of CO_2, leading to the consumption of CH generated during hydration and subsequent carbonation to form CC [69]. The blended cement paste demonstrated a higher degree of hydration compared to the control cement paste. This might be due to the porous nature of T-CCW, which absorbs and retains moisture, and a micro filler effect creating nucleation sites for the growth of hydration products within its pore structure [57].

4.4 Fourier Infrared Transform Spectroscopy

Fig. 15(d) presents the FTIR spectra of the paste samples cured for 7 days. Compared with the control sample (C0), no new absorption peaks were observed for the functional groups in the T-CCW blended samples. These observations are consistent with XRD results. The absorption peaks were observed at 3640, 3400, 1650, 1416, 1110, 950, and 870 cm^{-1} [66]. The absorption peak at 3640 cm^{-1} is attributed to the stretching vibration of OH in CH, and the broadband around 3400 cm^{-1} is associated with the stretching vibration of H_2O in hydration products, representing chemically bound water molecules in the hydration product [70]. The intensity of these bands decreases with increasing T-CCW, suggesting the presence of OH-phases. This could indicate the consumption of pozzolanic reactions. These findings correlate with the TGA-DTG curve calculated for the percentage of CH. The peak at 1650 cm^{-1} represents the hydroxyl group (H_2O) bending, indicating consistent amounts of bound water in all the mixes. At 1416 cm^{-1}, stretching vibrations of CO_3^{2-} suggest the presence of carbonate phases. The increase in peak intensity indicates a significant amount of CC in the carbonation products [71]. A minor peak at 1110 cm^{-1} corresponds to the sulphates (SO_4^{2-}), indicating the presence of AFt or AFm phases [72], which can be observed in SEM. The absorption peak at 950 cm^{-1} corresponds to Si-O stretching, indicating the hydration product C-S-H [73]. The intense band at 870 cm^{-1} is associated with the out-of-plane bending of CO_3^{2-} in carbonates [74], further supporting the increased carbonation in the samples.

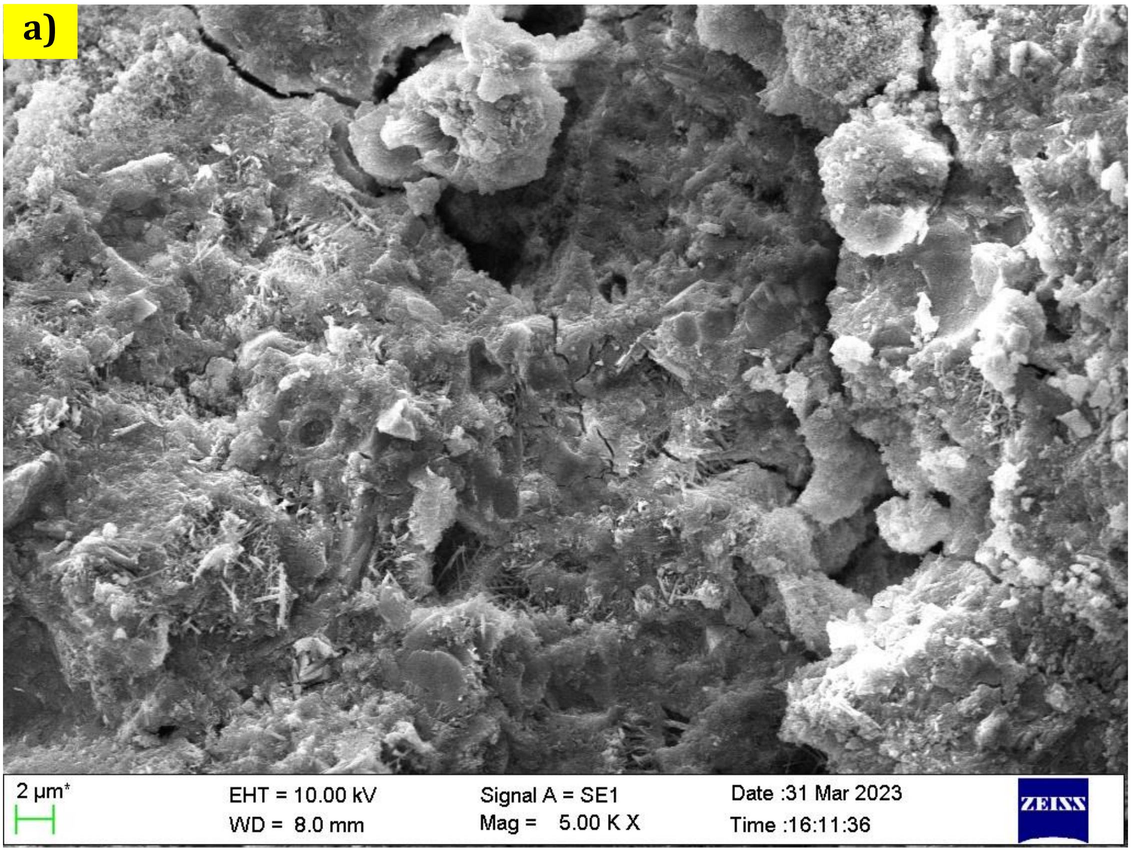
a)
2 µm*
EHT = 10.00 kV
WD = 8.0 mm
Signal A = SE1
Mag = 5.00 K X
Date :31 Mar 2023
Time :16:11:36
ZEISS

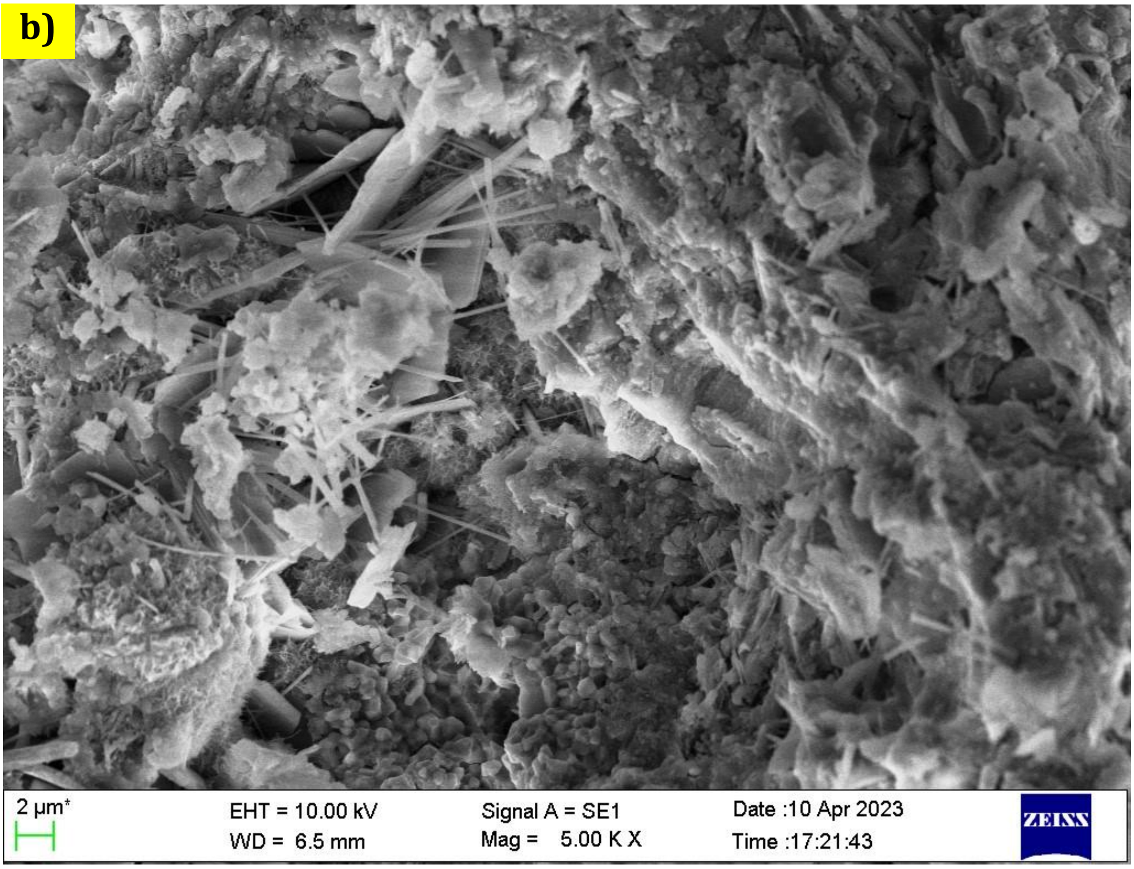
b)
2 µm*
EHT = 10.00 kV
WD = 6.5 mm
Signal A = SE1
Mag = 5.00 K X
Date :10 Apr 2023
Time :17:21:43
ZEISS

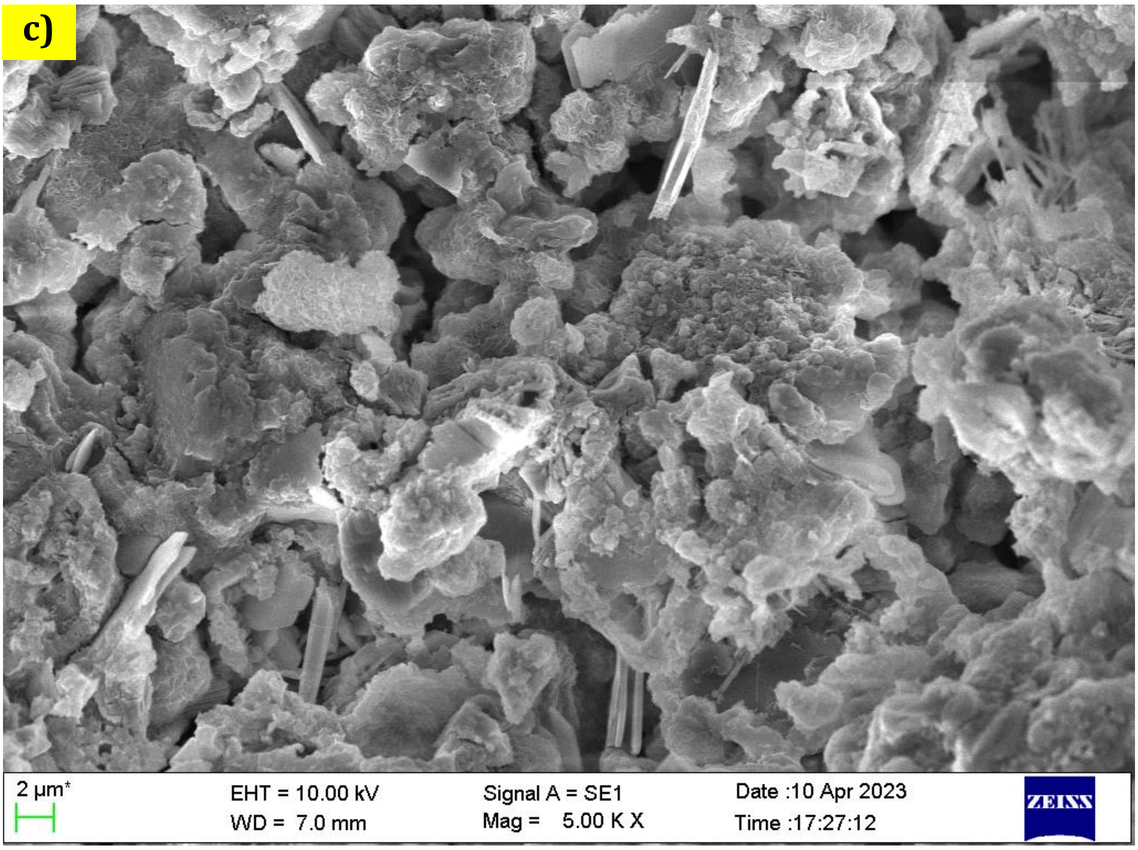

Fig. 14. SEM of the blended mixes at the T-CCW replacement of a) 0%, b) 10%, c) 25%

470

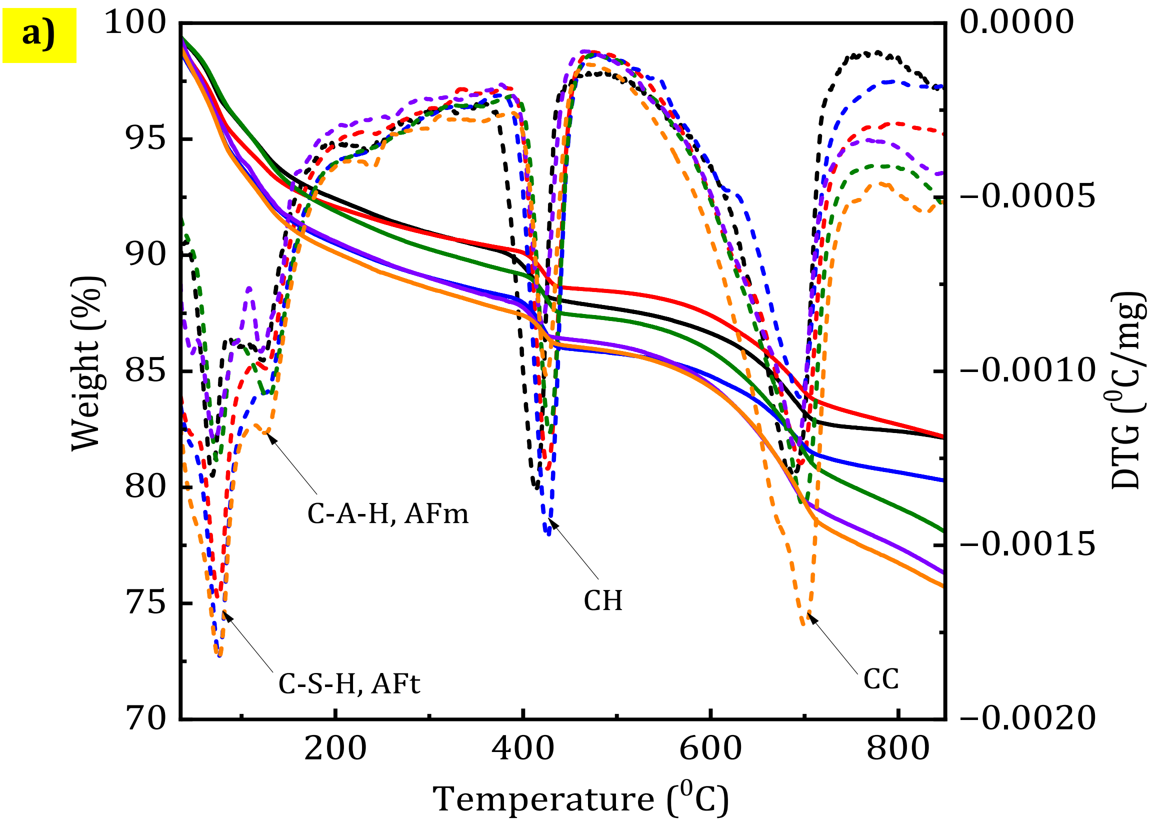

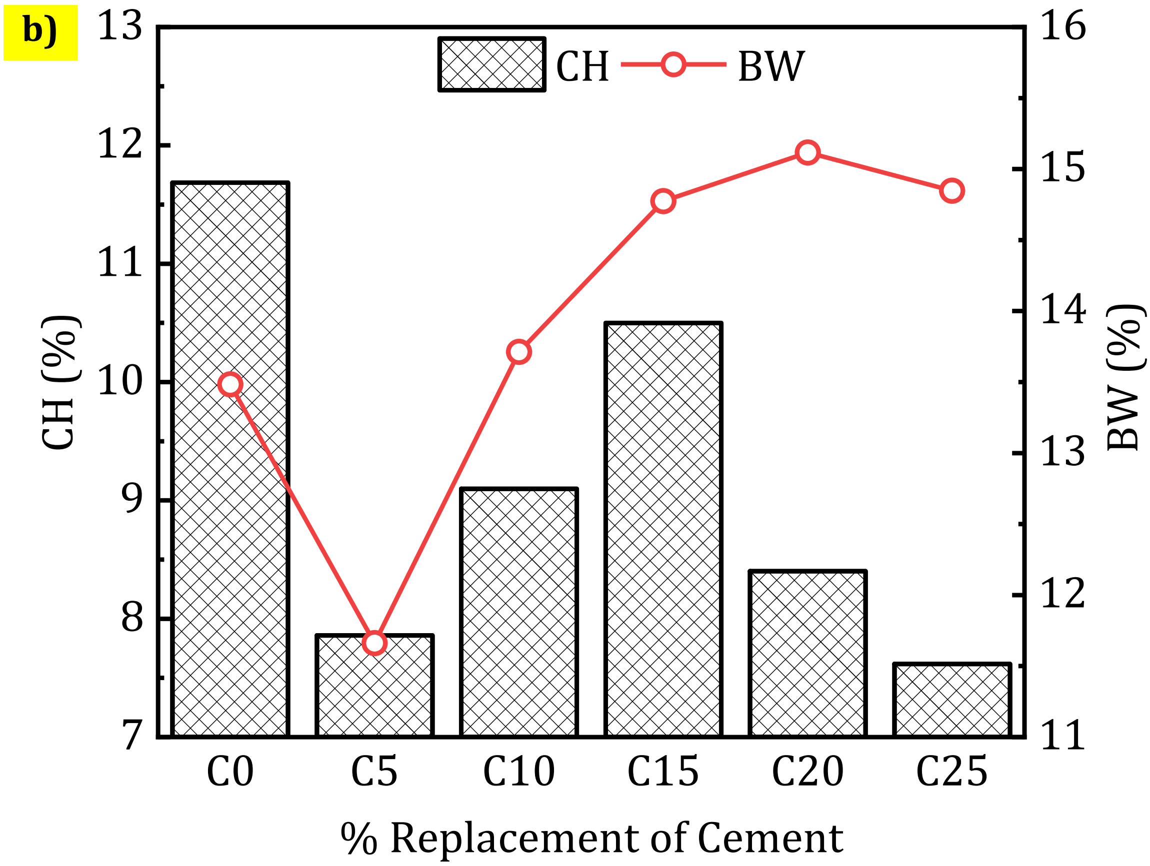
b)
CH
BW
CH (%)
BW (%)
13
12
11
10
9
8
7
16
15
14
13
12
11
C0
C5
C10
C15
C20
C25
% Replacement of Cement

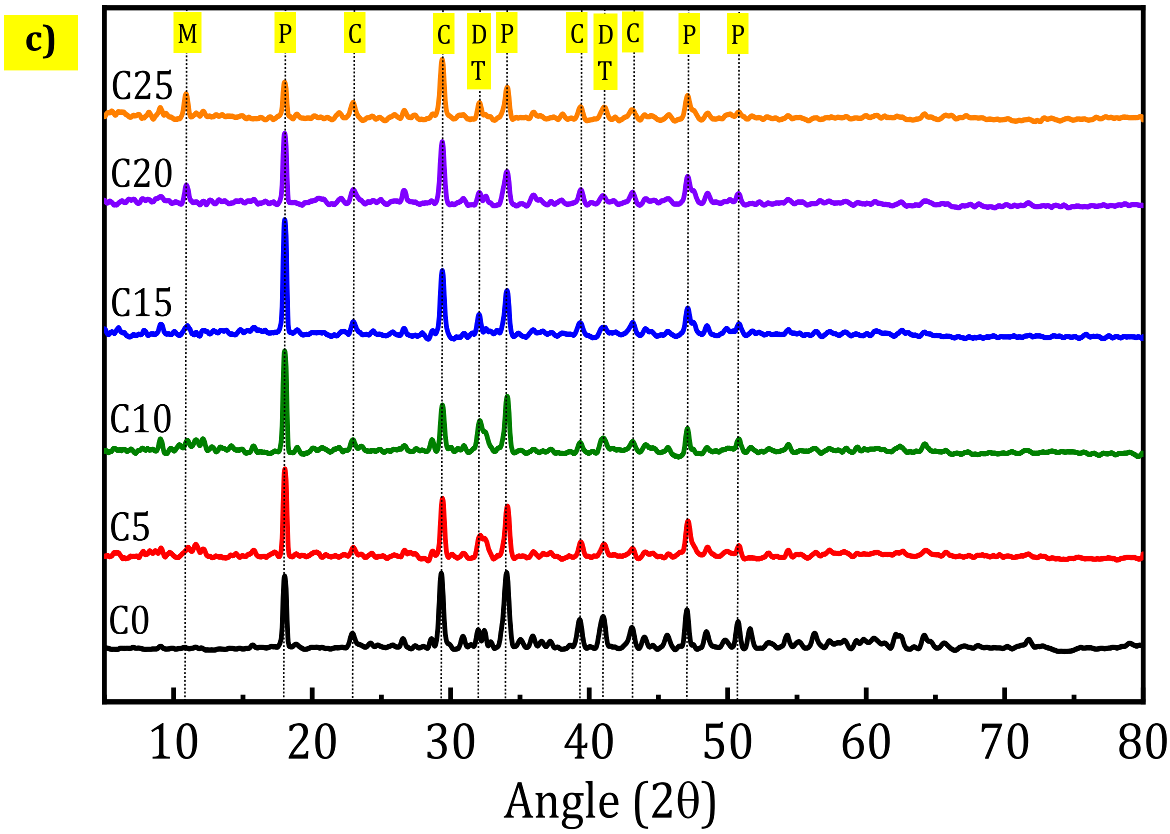
c)
M
P
C
C
D
T
P
C
D
T
C
P
P
C25
C20
C15
C10
C5
C0
10
20
30
40
50
60
70
80
Angle (2θ)

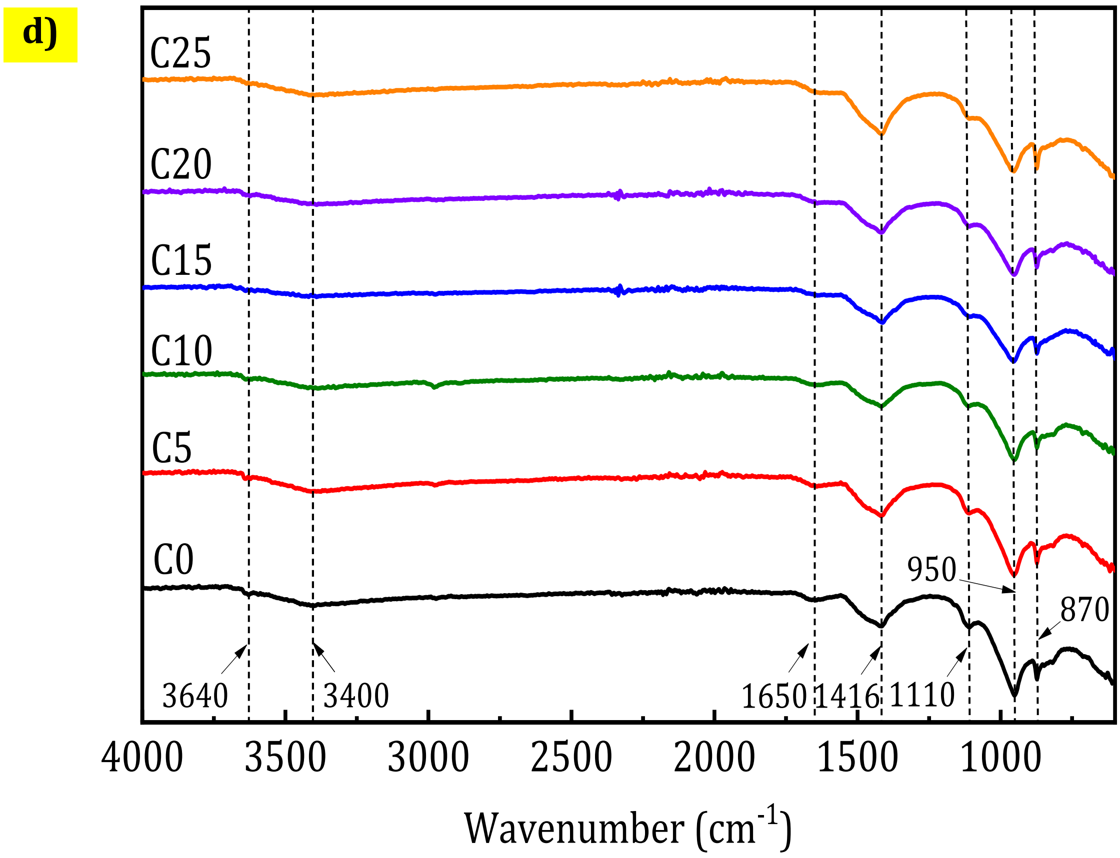

Fig. 15. a) TGA b) Percentage of BW and CH c) XRD d) FTIR of the blended pastes

5. Environmental Assessment

5.1 Sustainability Assessment

Researchers are exploring various alternative materials derived from industrial by-products and agricultural wastes in the search for sustainability in the construction industry. These materials not only substitute for conventional materials but also significantly lower the overall carbon footprint of the production. This approach addresses the pressing need for sustainable construction practices and tackles waste management challenges.

A simplified methodology is adopted to quantify the embodied carbon of the mortar mixes based on the summation of the embodied carbon of each material. The embodied carbon of the material, except T-CCW, was sourced from literature. The embodied carbon for cement is 0.931 [75], sand is 8.08 x 10^{-4} [75], and water is 1.12 x 10^{-4} [75]. Due to the unavailability of the embodied carbon for T-CCW from the literature, the CO_2 emission factors were analyzed by estimating the emission during T-CCW preparation, including transportation, drying, grinding, sieving, and calcination processes. The CO_2 emission factor for T-CCW is presented in Table 4. The embodied carbon assessment for the blended mortar was calculated for 1 kg of mortar using Eq. (3).

$$ECO_{2e} = \sum CO_{2i} \times W_i \quad (3)$$

Where CO_{2i} is the carbon factor, and W_i is the weight of each material used.

Table 4 Calculation of CO_2 emission factor for T-CCW

Material	Energy requirements for 1000 kg of T-CCW				Transportation of 1000 kg		Total emission (kg CO_2/kg)
	Consumption (kWh)			Emission factor (Kg CO_2/kWh)	Distance (Km)	Emission factor (kg CO_2/km)	
	Drying	Grinding and Sieving	Calcination				
T-CCW	25 [76]	174.6 [77]	12	0.79	150	0.148	0.189

Fig. 16 illustrates the embodied carbon of the blended mortar mixes. The control mix exhibits the highest embodied carbon of 0.44 kgCO_2/kg. The total embodied carbon decreased as the percentage of T-CCW increased. The embodied carbon of the blended mortar is 4%, 8%, 12%, 16%, and 20% lower than the control mortar. These results demonstrate that the addition of T-CCW as a partial replacement to cement substantially enhances the sustainability of the mortar mixes.

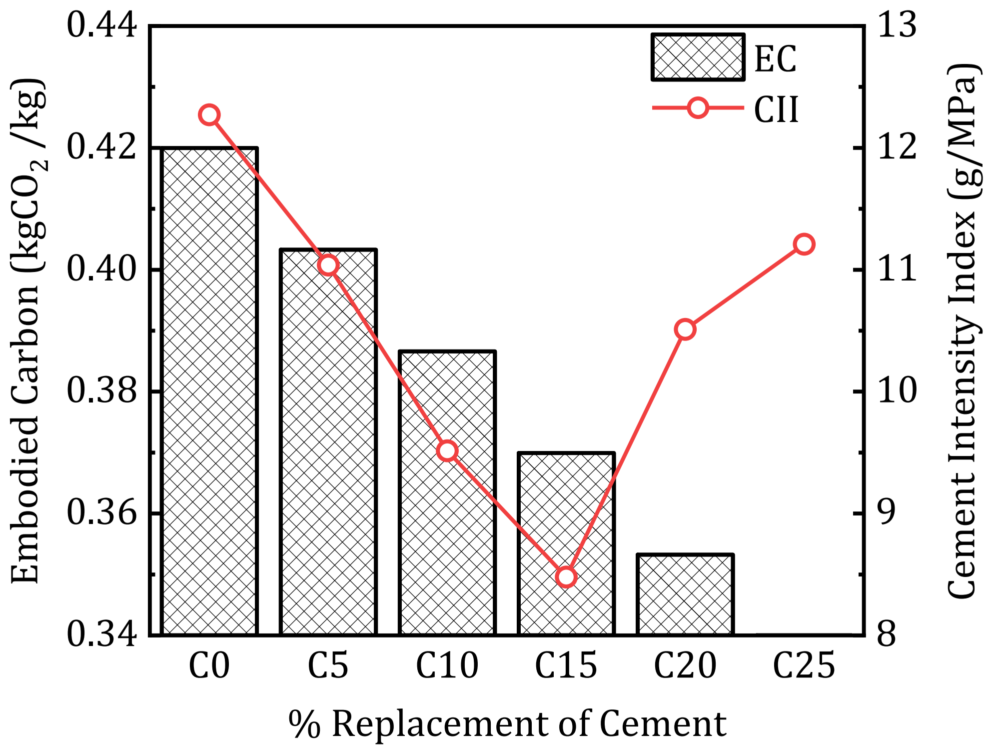

Fig. 16. Embodied carbon of blended mortars

In this study, CO_2 emission is the only environmental performance indicator used to demonstrate eco-friendliness. To reduce the carbon footprint of T-CCW, the recycling approach is to incorporate it into the mortar and mitigate the carbon emission of OPC. The cement content accounts for 26.67% of the mortar ratio of 1:2.75. Therefore, the CO_2 emission of cement in the control mortar is (0.2667 × 0.931) ≈ 0.2483 kgCO_2 per kg mortar. The CO_2 emission of T-CCW in the blended cement mortar, C25 is ((0.2667 × 0.75 × 0.931) + (0.2667 × 0.25 × 0.184)) ≈ 0.1974 kgCO_2 per kg mortar. Hence, the CO_2 reduction per kg of mortar is (0.2483 – 0.1974) ≈ 0.0509 kgCO_2 per kg mortar, approximately 20.5%. The amount of mortar produced with 1 tonne of T-CCW, 1 / (0.2667 × 0.25) ≈ 15 tonnes. The total CO_2 reduction per tonne of T-CCW is (0.0509 × 15000) ≈ 763.5 kgCO_2 ≈ 0.7635 tonnes CO_2. This approach primarily focuses on the direct carbon emission associated with material production. Further, a comprehensive environmental assessment is required from cradle to gate to provide a more holistic view of the material's environmental impact.

5.2 Cement Intensity Index

Fig. 16 presents the analysis of CII, indicating that the utilization of T-CCW as an alternative to cement in mortar necessitates less cement to attain a strength of 1 MPa compared to the control mix at 28 days. The control mortar exhibits a CII of 12.27 g/MPa, while the blended cement mortar shows lower values ranging from 8.48 to 11.21 g/MPa, with the C15 mix being the least compared to the control mortar, resulting in a saving of approximately 31% compared to control mortar. The results indicate that it is possible to produce quality mortar with comparable or better mechanical properties while significantly reducing cement content relative to the control mortar [78].

6. Factors affecting the utilization of T-CCW as a sustainable construction material

The fishbone diagram is a tool used to identify and explore the potential causes of a specific problem. It also provides ideas for future work to enhance further understanding of the problem. Fig. 17 presents a fishbone diagram illustrating the factors influencing the performance of CCWA as a cementitious composite. This visual representation summarizes the various parameters contributing to the effectiveness of CCWA in construction applications. The diagram outlines eight primary factors: raw material, mix design, curing, testing, environment, economy, and regulatory. These factors branch into sub-factors, highlighting the nature of developing and implementing CCWA-based cementitious materials. This overview serves as a roadmap for researchers and industry professionals, identifying key areas for investigation, optimization, and potential challenges in the development and application of CCWA-based cementitious composites. By addressing these factors, the potential of CCWA as a sustainable alternative as a construction material can be fully understood.

7. Conclusion

Reducing, reusing, and recycling are crucial to achieving sustainability. Exploring alternative materials from agricultural waste, such as CCW, generated from coffee processing addresses waste management challenges while decreasing the use of energy-intensive materials. This study examines the potential of T-CCW as a supplementary cementitious material, contributing to the development of sustainable construction practices. The following conclusions can be drawn from the study,

- The addition of T-CCW increased water demand for consistency, with water requirements increasing up to 46% compared to the control mix at 25% replacement.
- The high surface area and porous structure of T-CCW material provide nucleation sites for, and the water retention capacity of the T-CCW accelerated the setting times, with 25% replacement of T-CCW reducing initial and final setting times by 73% and 63%, respectively, compared to the control.
- The micro-filler effect and limited pozzolanic potential of T-CCW up to 15% improved the compressive strength of mortar at all curing ages compared to the control mix. The 15% T-CCW mix showed strength improvements of 82%, 53%, 49%, and 23% at 1, 3, 7, and 28 days respectively. The average compressive strength of T-CCW blended mortar was significantly higher than the current minimum strength required for the masonry units.
- UPV test results indicated improved homogeneity and compactness in all the blended cement mortars.
- Microstructural analysis showed that T-CCW enhances cement hydration and leads to denser microstructure through pozzolanic reaction and improved nucleation.
- Environmental analysis revealed that incorporating T-CCW reduced the embodied carbon of mortar mixes by 19% at 25% replacement.
- The cement intensity index was lowest for 15% T-CCW mix, indicating a 31% reduction in cement needed to achieve 1 MPa strength compared to the control.
- T-CCW can be used as a partial replacement for cement, with optimal performance at 15% replacement, contributing to cleaner production.

- Further research is needed to address various factors identified in the fishbone diagram to optimize the use of CCW in cementitious composites.
- Thus, this research shows the use of T-CCW as a sustainable material in cementitious composites when used in appropriate proportions.

Overall, incorporating T-CCW into mortar offers benefits across technical, economic, and environmental perspectives. Technically, CCW can potentially improve strength and microstructure properties. Economically, the use of T-CCW can lower material costs, reduce waste management expenses, and create new opportunities in the green construction market. Environmentally, utilization of T-CCW diverts waste from landfills, lowers the carbon footprint associated with mortar production, and conserves natural resources. Thus, this research shows the use of T-CCW as a sustainable material in cementitious composites when used in appropriate proportions.

The study was limited to a specific calcination temperature; hence, future research could investigate the effects of different calcination temperatures on the properties of CCW and its effectiveness in cementitious composites. Research is underway to determine the influence of T-CCW on the long-term durability properties, such as chemical attacks, carbonation, chloride ingress, and corrosion, and to extend the possibility of using T-CCW in structural concrete. Further, experimental work can be used to assess the leaching behaviour of T-CCW. Additionally, the research could explore the application of T-CCW in various types of concrete and its synergetic potential with other SCMs. Pilot scale trials and demonstrations are needed to validate the performance of T-CCW in real-world applications. Additionally, evaluating the economic feasibility and conducting a life cycle assessment of T-CCW production of large-scale production is essential for encouraging its widespread use. Addressing these limitations and pursuing these future research directions, significant progress can be made in optimizing the utilization of T-CCW and validating its suitability as an SCM in cementitious composites, thereby contributing to the circular economy strategies of the coffee processing industry.

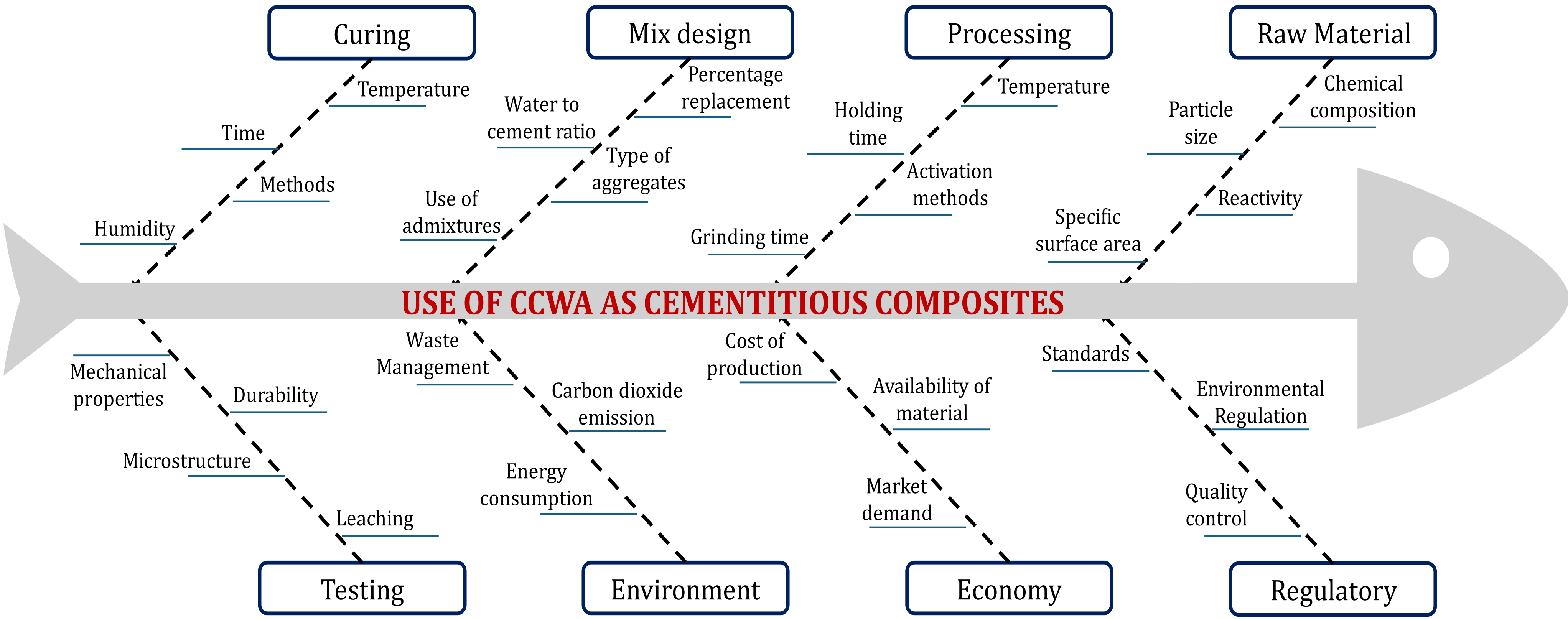

Fig. 17. Fishbone diagram

Credit authorship contribution statement

Balasubramanya Manjunath: Conceptualization, Investigation, Data curation, Validation, Formal analysis, Methodology, Visualization, Writing - original draft, Writing - review & editing. **Claudiane M. Ouellet-Plamondon:** Conceptualization, Data curation, Validation, Writing - review & editing. **Anjali Ganesh:** Writing - review & editing, Funding acquisition. **B.B. Das:** Data curation, Validation, Writing - review & editing. **Chandrasekhar Bhojaraju:** Conceptualization, Investigation, Data curation, Validation, Formal analysis, Methodology, Visualization, Supervision, Writing - original draft, Writing – review & editing, Funding acquisition.

Declaration of competing interest

The authors declare that they have no known competing financial interests or personal relationships that could have appeared to influence the work reported in this paper.

Data availability

No data was used for the research described in the article.

Acknowledgments

The authors thank the St Joseph Engineering College, Mangaluru, Karnataka, for their unwavering support during this research. The authors thank the technical staff and students for supporting our experiments. The authors acknowledge the Central Research Facility and Sustainable Construction and Building Materials Laboratory of the National Institute of Technology, Surathkal, Mangaluru, Karnataka, for SEM, XRD, TGA, and FTIR facility and National Centre for Earth Science Studies, Thiruvananthapuram, for the XRF and particle size analyzer facility for the study. The authors are grateful to the central instrumentation facility, Manipal Academy of Higher Education, Karnataka, for providing help with the SEM facility. Special thanks also to Amith R for his support in conducting the experiments.

Funding sources

This work was supported by the St Joseph Engineering College - Seed money grant [Grant Number: SJEC/DIR/B/2021/085]

Reference

1. Pierrehumbert, R., *There is no Plan B for dealing with the climate crisis.* Bulletin of the Atomic Scientists, 2019. **75**(5): p. 215-221.
2. Jokar, Z. and A. Mokhtar, *Policy making in the cement industry for CO2 mitigation on the pathway of sustainable development-A system dynamics approach.* Journal of Cleaner Production, 2018. **201**: p. 142-155.
3. Miller, S.A., A. Horvath, and P.J. Monteiro, *Readily implementable techniques can cut annual CO2 emissions from the production of concrete by over 20%.* Environmental Research Letters, 2016. **11**(7): p. 074029.
4. Environment, U., et al., *Eco-efficient cements: Potential economically viable solutions for a low-CO2 cement-based materials industry.* Cement and concrete Research, 2018. **114**: p. 2-26.
5. Nwankwo, C.O., et al., *High volume Portland cement replacement: A review.* Construction and Building materials, 2020. **260**: p. 120445.
6. WBCSD, I., *Cement Technology Roadmap 2009: carbon emissions reductions up to 2050.* World Business Council for Sustainable Development and International Energy Agency, 2009.
7. Chen, H., C.L. Chow, and D. Lau, *Developing green and sustainable concrete in integrating with different urban wastes.* Journal of Cleaner Production, 2022. **368**: p. 133057.
8. Chen, H. and J. Yang, *A new supplementary cementitious material: Walnut shell ash.* Construction and Building Materials, 2023. **408**: p. 133852.
9. Ruviaro, A.S., et al., *Characterization and investigation of the use of oat husk ash as supplementary cementitious material as partial replacement of Portland cement: Analysis of fresh and hardened properties and environmental assessment.* Construction and Building Materials, 2023. **363**: p. 129762.
10. Tekin, I., İ. Dirikolu, and H. Gökçe, *A regional supplementary cementitious material for the cement industry: Pistachio shell ash.* Journal of Cleaner Production, 2021. **285**: p. 124810.
11. Tavares, J.C., et al., *Use of banana leaf ash as partial replacement of Portland cement in eco-friendly concretes.* Construction and Building Materials, 2022. **346**: p. 128467.
12. Qudoos, A., H.G. Kim, and J.-S. Ryou, *Effect of mechanical processing on the pozzolanic efficiency and the microstructure development of wheat straw ash blended cement composites.* Construction and Building Materials, 2018. **193**: p. 481-490.
13. Cao, F., et al., *Effect of highland barley straw ash admixture on properties and microstructure of concrete.* Construction and Building Materials, 2022. **315**: p. 125802.
14. Wi, K., et al., *Use of an agricultural by-product, nano sized Palm Oil Fuel Ash as a supplementary cementitious material.* Construction and Building Materials, 2018. **183**: p. 139-149.
15. Munshi, S. and R.P. Sharma, *Investigation on the pozzolanic properties of rice straw ash prepared at different temperatures.* Materials Express, 2018. **8**(2): p. 157-164.
16. Bahurudeen, A., et al., *Performance evaluation of sugarcane bagasse ash blended cement in concrete.* Cement and Concrete Composites, 2015. **59**: p. 77-88.
17. Thiedeitz, M., B. Ostermaier, and T. Kränkel, *Rice husk ash as an additive in mortar–Contribution to microstructural, strength and durability performance.* Resources, Conservation and Recycling, 2022. **184**: p. 106389.
18. Shakouri, M., et al., *Hydration, strength, and durability of cementitious materials incorporating untreated corn cob ash.* Construction and Building Materials, 2020. **243**: p. 118171.
19. Shakouri, M., et al., *Pretreatment of corn stover ash to improve its effectiveness as a supplementary cementitious material in concrete.* Cement and Concrete Composites, 2020. **112**: p. 103658.
20. Manjunath, B., et al., *Potential utilization of regional cashew nutshell ash wastes as a cementitious replacement on the performance and environmental impact of eco-friendly mortar.* Journal of Building Engineering, 2023. **66**: p. 105941.

21. Forcina, A., et al., *A comparative life cycle assessment of different spent coffee ground reuse strategies and a sensitivity analysis for verifying the environmental convenience based on the location of sites.* Journal of Cleaner Production, 2023. **385**: p. 135727.
22. Jamora, J.B., et al., *Potential reduction of greenhouse gas emission through the use of sugarcane ash in cement-based industries: A case in the Philippines.* Journal of Cleaner Production, 2019. **239**: p. 118072.
23. Saberian, M., et al., *Recycling of spent coffee grounds in construction materials: A review.* Journal of Cleaner Production, 2021. **289**: p. 125837.
24. Ayseli, M.T., H. Kelebek, and S. Selli, *Elucidation of aroma-active compounds and chlorogenic acids of Turkish coffee brewed from medium and dark roasted Coffea arabica beans.* Food chemistry, 2021. **338**: p. 127821.
25. Lima, F., T. Gomes, and J. Moraes, *Effect of coffee husk ash as alkaline activator in one-part alkali-activated binder.* Construction and Building Materials, 2023. **362**: p. 129799.
26. Dhull, S.B., A. Singh, and P. Kumar, *Food Processing Waste and Utilization: Tackling Pollution and Enhancing Product Recovery*. 2022: CRC Press/Taylor & Francis Group.
27. Cruz, R., *Coffee by-products: sustainable agro-industrial recovery and impact on vegetables quality.* 2014.
28. Oussou, K.F., et al., *Valorization of cocoa, tea and coffee processing by-products-wastes.* 2023.
29. Murthy, P.S. and M.M. Naidu, *Sustainable management of coffee industry by-products and value addition—A review.* Resources, Conservation and recycling, 2012. **66**: p. 45-58.
30. Janissen, B. and T. Huynh, *Chemical composition and value-adding applications of coffee industry by-products: A review.* Resources, Conservation and recycling, 2018. **128**: p. 110-117.
31. Nolasco, A., et al., *Valorization of coffee industry wastes: Comprehensive physicochemical characterization of coffee silverskin and multipurpose recycling applications.* Journal of cleaner production, 2022. **370**: p. 133520.
32. Vieira, T., S. Cunha, and S. Casal, *Mycotoxins in coffee*, in *Coffee in health and disease prevention*. 2015, Elsevier. p. 225-233.
33. Bahurudeen, A. and M. Santhanam, *Influence of different processing methods on the pozzolanic performance of sugarcane bagasse ash.* Cement and Concrete Composites, 2015. **56**: p. 32-45.
34. Lin, L.-K., T.-M. Kuo, and Y.-S. Hsu, *The application and evaluation research of coffee residue ash into mortar.* Journal of Material Cycles and Waste Management, 2016. **18**: p. 541-551.
35. Hakeem, I.Y., et al., *Effects of nano sized sesame stalk and rice straw ashes on high-strength concrete properties.* Journal of Cleaner Production, 2022. **370**: p. 133542.
36. Caronge, M.A., et al., *Feasibility study on the use of processed waste tea ash as cement replacement for sustainable concrete production.* Journal of Building Engineering, 2022. **52**: p. 104458.
37. Bhojaraju, C., et al., *Fresh and hardened properties of GGBS-contained cementitious composites using graphene and graphene oxide.* Construction and Building Materials, 2021. **300**: p. 123902.
38. John, V.M., et al., *Rethinking cement standards: Opportunities for a better future.* Cement and Concrete Research, 2019. **124**: p. 105832.
39. Bhojaraju, C., M. Di Mare, and C.M. Ouellet-Plamondon, *The impact of carbon-based nanomaterial additions on the hydration reactions and kinetics of GGBS-modified cements.* Construction and Building Materials, 2021. **303**: p. 124366.
40. Deboucha, W., et al., *Hydration development of mineral additives blended cement using thermogravimetric analysis (TGA): Methodology of calculating the degree of hydration.* Construction and Building Materials, 2017. **146**: p. 687-701.
41. Le, T.-T., et al., *Strength characteristics of spent coffee grounds and oyster shells cemented with GGBS-based alkaline-activated materials.* Construction and Building Materials, 2021. **267**: p. 120986.

42. Yusuf, M.O., et al., *Strength and Microstructure of Coffee Silverskin Blended Mortar.* Recycling, 2022. **7**(4): p. 59.
43. Craig, A.P., A.S. Franca, and L.S. Oliveira, *Discrimination between defective and non-defective roasted coffees by diffuse reflectance infrared Fourier transform spectroscopy.* Lwt, 2012. **47**(2): p. 505-511.
44. Pujol, D., et al., *The chemical composition of exhausted coffee waste.* Industrial Crops and Products, 2013. **50**: p. 423-429.
45. Figueiró, S., et al., *On the physico-chemical and dielectric properties of glutaraldehyde crosslinked galactomannan–collagen films.* Carbohydrate polymers, 2004. **56**(3): p. 313-320.
46. Pudjiastuti, L., et al. *Lignocellulosic properties of coffee pulp waste after alkaline hydrogen peroxide treatment*. in *IOP Conference Series: Materials Science and Engineering*. 2019. IOP Publishing.
47. Kloss, S., et al., *Characterization of slow pyrolysis biochars: effects of feedstocks and pyrolysis temperature on biochar properties.* Journal of environmental quality, 2012. **41**(4): p. 990-1000.
48. Ben Abdallah, A., et al., *Pyrolysis of tea and coffee wastes: effect of physicochemical properties on kinetic and thermodynamic characteristics.* Journal of Thermal Analysis and Calorimetry, 2023. **148**(6): p. 2501-2515.
49. Polat, S. and P. Sayan, *Assessment of the thermal pyrolysis characteristics and kinetic parameters of spent coffee waste: a TGA-MS study.* Energy Sources, Part A: Recovery, Utilization, and Environmental Effects, 2023. **45**(1): p. 74-87.
50. Li, S. and G. Chen, *Thermogravimetric, thermochemical, and infrared spectral characterization of feedstocks and biochar derived at different pyrolysis temperatures.* Waste Management, 2018. **78**: p. 198-207.
51. NF, P., *P 18–513; Additions for Concrete—Metakaolin—Specifications and Conformity Criteria.* Afnor: Paris, France, 2012.
52. Khan, K., et al., *Effect of fineness of basaltic volcanic ash on pozzolanic reactivity, ASR expansion and drying shrinkage of blended cement mortars.* Materials, 2019. **12**(16): p. 2603.
53. Tan, K., et al., *Properties of cement mortar containing pulverized biochar pyrolyzed at different temperatures.* Construction and Building Materials, 2020. **263**: p. 120616.
54. Gupta, S. and H.W. Kua, *Carbonaceous micro-filler for cement: Effect of particle size and dosage of biochar on fresh and hardened properties of cement mortar.* Science of the Total Environment, 2019. **662**: p. 952-962.
55. Bu, Y. and J. Weiss, *The influence of alkali content on the electrical resistivity and transport properties of cementitious materials.* Cement and Concrete Composites, 2014. **51**: p. 49-58.
56. Gedefaw, A., et al., *Experimental investigation on the effects of coffee husk ash as partial replacement of cement on concrete properties.* Advances in Materials Science and Engineering, 2022. **2022**(1): p. 4175460.
57. Gupta, S., H.W. Kua, and H.J. Koh, *Application of biochar from food and wood waste as green admixture for cement mortar.* Science of the total environment, 2018. **619**: p. 419-435.
58. Gupta, S., H.W. Kua, and C.Y. Low, *Use of biochar as carbon sequestering additive in cement mortar.* Cement and concrete composites, 2018. **87**: p. 110-129.
59. Li, Q., et al., *Effect of waste corn stalk ash on the early-age strength development of fly ash/cement composite.* Construction and Building Materials, 2021. **303**: p. 124463.
60. Banu, S.S., J. Karthikeyan, and P. Jayabalan, *Effect of agro-waste on strength and durability properties of concrete.* Construction and Building Materials, 2020. **258**: p. 120322.
61. Roychand, R., et al., *Transforming spent coffee grounds into a valuable resource for the enhancement of concrete strength.* Journal of cleaner production, 2023. **419**: p. 138205.
62. Siddique, R., *Performance characteristics of high-volume Class F fly ash concrete.* Cement and Concrete Research, 2004. **34**(3): p. 487-493.
63. Oner, A. and S. Akyuz, *An experimental study on optimum usage of GGBS for the compressive strength of concrete.* Cement and concrete composites, 2007. **29**(6): p. 505-514.

64. Malhotra, V.M. and N.J. Carino, *Handbook on nondestructive testing of concrete*. 2003: CRC press.
65. Yang, X. and X.-Y. Wang, *Hydration-strength-durability-workability of biochar-cement binary blends.* Journal of Building Engineering, 2021. **42**: p. 103064.
66. Javed, M.H., et al., *Effect of various biochars on physical, mechanical, and microstructural characteristics of cement pastes and mortars.* Journal of Building Engineering, 2022. **57**: p. 104850.
67. Ali, D., et al., *Thermo-physical properties and microstructural behaviour of biochar-incorporated cementitious material.* Journal of Building Engineering, 2023. **64**: p. 105695.
68. Maljaee, H., et al., *Effect of cement partial substitution by waste-based biochar in mortars properties.* Construction and Building Materials, 2021. **301**: p. 124074.
69. Šavija, B. and M. Luković, *Carbonation of cement paste: Understanding, challenges, and opportunities.* Construction and Building Materials, 2016. **117**: p. 285-301.
70. Wang, L., et al., *Eco-friendly treatment of recycled concrete fines as supplementary cementitious materials.* Construction and Building Materials, 2022. **322**: p. 126491.
71. Chen, X., et al., *Sludge biochar as a green additive in cement-based composites: Mechanical properties and hydration kinetics.* Construction and Building Materials, 2020. **262**: p. 120723.
72. Yang, X., et al., *Behavior of biochar-modified cementitious composites exposed to high temperatures.* Materials, 2021. **14**(18): p. 5414.
73. Yang, X. and X.-Y. Wang, *Strength and durability improvements of biochar-blended mortar or paste using accelerated carbonation curing.* Journal of CO2 Utilization, 2021. **54**: p. 101766.
74. Hughes, T.L., et al., *Determining cement composition by Fourier transform infrared spectroscopy.* Advanced Cement Based Materials, 1995. **2**(3): p. 91-104.
75. Yang, K.-H., S.-H. Tae, and D.-U. Choi, *Mixture Proportioning Approach for Low-CO 2 Concrete Using Supplementary Cementitious Materials.* ACI Materials Journal, 2016. **113**(4).
76. Alnahhal, M.F., et al., *Assessment on engineering properties and CO2 emissions of recycled aggregate concrete incorporating waste products as supplements to Portland cement.* Journal of cleaner production, 2018. **203**: p. 822-835.
77. Tantri, A., et al., *Implementation assessment of calcined and uncalcined cashew nut-shell ash with total recycled concrete aggregate in self-compacting concrete employing Bailey grading technique.* Innovative Infrastructure Solutions, 2022. **7**(5): p. 305.
78. Bhagithimar, Y., et al., *Development of sustainable conductive cementitious composite using graphite-coated spent catalyst waste.* Journal of Building Engineering, 2024. **93**: p. 109864.